Journal of Experimental Marine Biology and Ecology 498 (2018) 46–60

Contents lists available at ScienceDirect

Journal of Experimental Marine Biology and Ecology

journal homepage: www.elsevier.com/locate/jembe

Ocean acidification impacts primary and bacterial production in Antarctic coastal waters during austral summer

K.J. Westwood[a,b,c,*], P.G. Thomson[d], R.L. van den Enden[a], L.E. Maher[e], S.W. Wright[a,b,c], A.T. Davidson[a,b,c]

[a] Department of the Environment and Energy, Australian Antarctic Division, 203 Channel Highway, Kingston, Tasmania 7050, Australia
[b] Antarctic Climate and Ecosystems Cooperative Research Centre (ACE CRC), University of Tasmania, Private Bag 80, Hobart, Tasmania 7001, Australia
[c] Institute of Marine and Antarctic Studies (IMAS), University of Tasmania, Private Bag 129, Hobart, Tasmania 7001, Australia
[d] School of Environmental Systems Engineering, The UWA Oceans Institute, The University of Western Australia, Mailstop 470, 35 Stirling Highway, Crawley, Western Australia 6009, Australia
[e] City of Hobart, Town Hall, Macquarie Street, GPO Box 503, Hobart, Tasmania 7001, Australia

ARTICLE INFO

Keywords:
Ocean acidification
Primary production
Bacterial production
Net community production
Photosynthesis
Antarctica

ABSTRACT

Polar waters may be highly impacted by ocean acidification (OA) due to increased solubility of CO_2 at colder water temperatures. Three experiments examining the influence of OA on primary and bacterial production were conducted during austral summer at Davis Station, East Antarctica (68°35′ S, 77°58′ E). For each experiment, six minicosm tanks (650 L) were filled with 200 µm filtered coastal seawater containing natural communities of Antarctic marine microbes. Assemblages were incubated for 10 to 12 days at CO_2 concentrations ranging from pre-industrial to post-2300. Primary and bacterial production rates were determined using $NaH^{14}CO_3$ and ^{14}C-leucine, respectively. Net community production (NCP) was also determined using dissolved oxygen. In all experiments, maximum photosynthetic rates (P_{max}, mg C mg chl a^{-1} h^{-1}) decreased with elevated CO_2, clearly reducing rates of total gross primary production (mg C L^{-1} h^{-1}). Rates of cell-specific bacterial productivity (µg C $cell^{-1}$ h^{-1}) also decreased under elevated CO_2, yet total bacterial production (µg C L^{-1} h^{-1}) and cell abundances increased with CO_2 over Days 0–4. Initial increases in bacterial production and abundance were associated with fewer heterotrophic nanoflagellates and therefore less grazing pressure. The main changes in primary and bacterial productivity generally occurred at CO_2 concentrations > 2 × present day (> 780 ppm), with the same responses occurring regardless of seasonally changing environmental conditions and microbial assemblages. However, NCP varied both within and among experiments, largely due to changing nitrate + nitrite (NOx) availability. At NOx concentrations < 1.5 µM photosynthesis to respiration ratios showed that populations switched from net autotrophy to heterotrophy and CO_2 responses were suppressed. Overall, OA may reduce production in Antarctic coastal waters, thereby reducing food availability to higher trophic levels and reducing draw-down of atmospheric CO_2, thus forming a positive feedback to climate change. NO_X limitation may suppress this OA response but cause a similar decline.

1. Introduction

Polar regions are vulnerable to ocean acidification (OA) due to the high solubility of CO_2 in colder waters (Sarmiento et al., 2004). However, the effects on marine organisms are difficult to predict given the wide-ranges of responses between studies (Liu et al., 2010). Experimental outcomes have largely depended on species-specific differences in physiology, timescales of responses measured, acclimation state and study duration, the rate and magnitude of the CO_2 perturbation, and the method used to alter pH (Riebesell et al., 2008; Hurd et al., 2009). Responses can also depend on the scale of the work undertaken, ranging from single-species experiments in the laboratory (*e.g.* Gattuso and Hansson, 2011), up to large scale mesocosm enclosures where interactions between various components of the food web are able to be assessed *in situ* (*e.g.* Pelagic Ecosystem CO_2 Enrichment Studies I, II, III, PeECE, Riebesell et al., 2007, 2008; European Project on Ocean Acidification, EPOCA, Riebesell et al., 2013). In Antarctic waters, larger-scale experimental work to evaluate OA impacts across different trophic levels (*i.e.* community responses) are lacking.

Antarctic coastal communities may show high tolerances to OA due

* Corresponding author at: Department of the Environment and Energy, Australian Antarctic Division, 203 Channel Highway, Kingston, Tasmania 7050, Australia.
E-mail addresses: Karen.Westwood@aad.gov.au (K.J. Westwood), paul.thomson@uwa.edu.au (P.G. Thomson), Rick.Vandenenden@aad.gov.au (R.L. van den Enden), maherl@hobartcity.com.au (L.E. Maher), Simon.Wright@aad.gov.au (S.W. Wright), Andrew.Davidson@aad.gov.au (A.T. Davidson).

https://doi.org/10.1016/j.jembe.2017.11.003
Received 20 December 2016; Received in revised form 10 October 2017; Accepted 11 November 2017
Available online 20 November 2017
0022-0981/ Crown Copyright © 2017 Published by Elsevier B.V. All rights reserved.

to large seasonal fluctuations of CO_2 that occur *in situ* (Gibson and Trull, 1999; Roden et al., 2013; Tortell et al., 2014). Naturally high concentrations up to 450 ppm (atmospheric concentrations 390 ppm during this study) occur under the sea-ice in winter between July and September due to biological remineralisation and the absence of photosynthesis during the aphotic winter, upwelling of CO_2-rich deep water at the shelf break, and sea-ice obstructing the exchange of CO_2 with the atmosphere (Gibson and Trull, 1999; Davidson et al., 2016). At the onset of spring in October, CO_2 drastically declines with concentrations often falling to < 100 ppm under the sea-ice by December (Gibson and Trull, 1999; Tortell et al., 2014). Low CO_2 is largely the result of increased photosynthesis associated with sea-ice melt and increased light availability, but is also partially the result of the meltwater itself characterised by low dissolved inorganic carbon (Gleitz et al., 1995; Gibson and Trull, 1999; Tortell et al., 2014). During summer when sea-ice is absent (January, February), CO_2 is generally within the range of 100 to 200 ppm, still well below atmospheric concentrations and indicating that air-sea fluxes of CO_2 are insufficient to counteract biological activity (Gibson and Trull, 1999). Overall, seasonal changes in CO_2 concentrations may expose communities to fluctuations > 350 ppm.

The marine microbial loop plays a pivotal role in controlling carbon uptake and export in Antarctic waters through the biological pump (Ducklow et al., 2001; Deppeler and Davidson, 2017), and provides energy to higher trophic levels (*e.g.* krill) within the Antarctic food web (Nicol et al., 2010). The effects of OA on all facets of the Antarctic marine microbial loop require detailed assessment. Phytoplankton responses to OA in previous studies have included (but not consistently) increased primary production and growth (Hein and Sand-Jensen, 1997; Tortell et al., 2008; Egge et al., 2009; Trimborn et al., 2013), decreased calcification (Delille et al., 2005), and increased carbon consumption relative to other elements (Toggweiler, 1993; Riebesell et al., 2007; Bellerby et al., 2008). Increased production and growth have been associated with the down-regulation carbon concentrating mechanisms which are energetically costly (Mackey et al., 2015). However, in Antarctic waters the down-regulation of CCMs does not always imply increased growth due to reduced energetic requirements to concentrate CO_2 and saturate Ribulose-1,5-bisphosphate carboxylase/oxygenase (Rubisco) at low temperatures (Kranz et al., 2015; Young et al., 2015). The expression of OA responses may also be modified by interacting factors such as light and iron availability (Gao et al., 2012; Hoppe et al., 2013; Boyd et al., 2015; Hoppe et al., 2015; Trimborn et al., 2017). At the community level, OA has been shown to cause shifts from large to small (> 5 μm) phytoplankton cells, in both Antarctic and Arctic waters (Davidson et al., 2016; Thomson et al., 2016; Brussaard et al., 2013; Riebesell et al., 2013; Schulz et al., 2013). This may influence carbon export through slowed sinking rates, as well as food availability for krill due to inefficient filtering (Boyd et al., 1984; Kawaguchi et al., 1999; Davidson et al., 2016).

Bacterial responses to OA have varied according to studies in different regions. In temperate systems, responses have included increased production and extracellular enzyme activity (Grossart et al., 2006), increased diversity (Allgaier et al., 2008), but no change in abundance (Grossart et al., 2006; Allgaier et al., 2008). In Antarctic waters, Thomson et al. (2016) found increased abundances of bacteria with OA, attributed to decreased grazing by heterotrophic nanoflagellates (see also this study). Maas et al. (2013) also found increased bacterial abundances and extracellular enzyme activity. These increases were due to the rapid evolution of bacterial populations, but diversity was significantly reduced. In an Arctic mesocosm experiment (Riebesell et al., 2013), OA increased both primary and dissolved organic carbon production, allowing a subsequent increase in bacterial production after a short lag phase (Engel et al., 2013; Piontek et al., 2013). Bacterial extracellular enzyme activity and viral abundances also increased with OA, which may affect remineralisation of organic matter and thus carbon export (Brussaard et al., 2013; Piontek et al., 2013).

We assessed the effects of OA on the Antarctic marine microbial loop using natural communities incubated in minicosm tanks (650 L) under controlled conditions. Given the large range of CO_2 concentrations that are known to occur *in situ* in Antarctic waters, we aimed to elucidate the 'tipping-point' where OA impacts may take effect, and how this may change throughout the season in response to changing environmental conditions and microbial community composition. To address our aim we conducted three dose-response experiments during early-, mid- and late-summer. Based on previous studies, our hypothesis was that primary and bacterial production would be stimulated under OA conditions due to increased carbon availability, with the extent of responses likely to change over the season.

2. Methods

Three experiments were conducted during austral summer at Davis Station, East Antarctica (68°35′ S, 77°58′ E), each of 10 to 12 days duration. The first experiment commenced on 30th December (early-summer), two weeks after the sea-ice had broken out. The second experiment commenced on 20th January (mid-summer), and the third experiment on 9th February (late-summer). Experiments were conducted in 6 × 650 L minicosm tanks housed in a temperature-regulated reefer container located on the coast (see also Davidson et al., 2016). All tanks were filled simultaneously with seawater collected from 60 m offshore at 2 m depth using a diaphragm pump. The seawater was filtered through 200 μm mesh to remove large grazers. Cells were kept suspended in the tanks by constant mixing with a shielded rotating auger at 15 rpm. The temperature of the tanks was maintained to within ± 0.1 °C of *in situ* measurements at the time of filling. This was achieved by cooling of the reefer, offset against warming of the filled tanks using 300 W aquarium heaters (Fluval). Illumination of tanks was from 4:00 to 23:00 local time (19 h light) with 5 h dark, using 150 W metal-halide lamps (Osram) covered with CT Blue filter to represent *in situ* wavelengths. Light availability was measured in empty tanks prior to experimentation at three depths (top 0 m, middle 0.55 m, near-bottom 0.91 m) and across each tank (right, middle, left) using a spherical LICOR PAR sensor. All tanks were dosed with 5 nM Na[Fe (EDTA)].$3H_20$ at the start of experimentation to alleviate potential iron limitation. However, it is unclear as to whether the iron was bioavailable due to the complexities of iron biogeochemistry (Hassler and Schoemann, 2009). Each minicosm tank had a teflon ball-valve tap with an inward protruding tube to enable sampling. A silicon hose was connected to the outside of the tap for the gentle filling of sampling containers. Samples were taken at 08:00 every 2 days.

2.1. CO_2 dosing

Target CO_2 treatments for the early-summer experiment ranged from ambient (control) to post-2300 (Caldeira and Wickett, 2003). In the early-summer experiment, concentrations in the tanks were maintained at × 0.2 (ambient control), × 1.6, × 3.2, × 4.8 or × 6.1 present day atmospheric concentrations (390 ppm at the time of experimentation). This corresponded to 78, 624, 1248, 1872 and 2379 ppm CO_2 for each treatment, respectively. For the mid- and late-summer experiments, the range of treatments was narrowed, with concentrations in the tanks maintained at × 0.5 (ambient control), × 1, × 2, × 3 or × 4 present day. This corresponded to 195, 390, 780, 1170 and 1560 ppm CO_2, respectively. For all control treatments, tanks were filled with ambient seawater and left untreated on Day 0 (ambient CO_2 concentrations were low following ice melt and spring blooms). Additional CO_2 was then added to the control tanks throughout experimentation as photosynthesis progressed, to maintain initial ambient CO_2 conditions. For non-control treatments, CO_2 was added to the tanks on the same day as filling.

CO_2 manipulations in the tanks conformed to recommendations in the "Guide to Best Practices for Ocean Acidification Research and Data

Reporting" (Riebesell et al., 2010). To obtain the required CO_2 treatments described above, tanks were dosed over 2 h with appropriate volumes of CO_2-saturated seawater obtained through bubbling with pure gas. CO_2 was added to tanks daily to maintain target concentrations during experiments. Carbonate chemistry was constrained through measurements of pH, alkalinity, temperature, salinity and atmospheric pressure. The maximum volume of CO_2 saturated seawater added to any 650 L tank over the course of an experiment was 3.1 L. As this was approximately 0.5% of the total tank volume there were no dilution factors applied to cell concentrations.

The experimental design was limited by having only six minicosm tanks. It was decided to test a range of CO_2 concentrations with little replication rather than two concentrations with three replicates. This was to allow the determination of a physiological tipping point for CO_2 effects, with the ranges allowing a dose-response curve. The lack of replication across treatments meant that rigorous statistical analyses were unable to be conducted. However, the × 4.8 or × 3 treatments were duplicated for each experiment and showed remarkably similar responses throughout. In addition, primary and bacterial productivity responses showed consistent trends among CO_2 treatments for every experiment over summer. We therefore believe that our data adequately represented the effects of CO_2 on the microbial community despite lack of replication within experiments, and that the results were not due to random variation.

2.2. Oxygen measurements

Dissolved oxygen was measured at one minute intervals in the tanks using optically isolated dipping probes (fibre-optic minisensors) connected to a four-channel (Oxy-4) meter system (PreSens GmbH). As there were six tanks but only four probes, the treatments monitored were × 0.2, × 3.2, × 4.8A and × 6.1 in the early-summer experiment, and × 0.5, × 2, × 3A and × 4 in the mid- and late-summer experiments. All data were corrected for temperature and salinity. Rates of change in oxygen concentration with time were determined through least-squares linear regression. Positive slopes determined from data measured during the day (19 h light) reflected net community production (NCP). Negative slopes determined from data measured during the night (5 h dark) reflected respiration. Gross primary production (GPP) rates over 24 h were calculated from the addition of NCP and respiration rates. Photosynthesis to respiration (P:R) ratios were calculated through the division of GPP by respiration. As the minicosm tanks were sealed there were no corrections for the flux of oxygen between water contained within the tanks and the overlying headspace. Data from the first two days of experimentation were excluded from analyses due to the possibility that oxygen had not yet equilibrated.

2.3. ^{14}C uptake

Rates of phytoplankton photosynthesis were determined for each treatment every 2 days using $NaH^{14}CO_3$ uptake. Incubations were conducted in the laboratory according to the method of Westwood et al. (2011), for 1 h under 21 light intensities ranging from 0 to 250 μmol m^{-2} s^{-1}. Carbon uptake rates were corrected for chlorophyll *a* (chl *a*) concentrations in the tanks measured using high performance liquid chromatography (HPLC, Wright et al., 2010) and for total dissolved inorganic carbon availability (Davidson et al., 2016). Photosynthesis-irradiance (P–I) relationships were then plotted and analysed using SYSTAT 8.0. The equation of Platt et al. (1980) was used to fit curves to the data using least squares non-linear regression. Photosynthesis parameters determined included the light-saturated photosynthetic rate [P_{max}, mg C (mg chl *a*)$^{-1}$ h^{-1}]; the photosynthetic efficiency [initial slope of the light-limited section of the P–I curve, α, mg C (mg chl *a*)$^{-1}$ h^{-1} (μmol m^{-2} s^{-1})$^{-1}$]; and the light intensity at which carbon-uptake became maximal (E_k, μmol m^{-2} s^{-1}), calculated as P_{max}/α. Light was not limiting to phytoplankton in the tanks at any time during experimentation despite increasing chlorophyll concentrations (see Section 3.1). Therefore, final total gross primary production rates (GPP, mg C L^{-1} h^{-1}) were calculated from modelled P_{max} values and chlorophyll [*i.e.* P_{max}, mg C (mg chl *a*)$^{-1}$ h^{-1} ∗ chlorophyll, μg chl *a* L^{-1} = GPP, mg C L^{-1} h^{-1}]. P_{max} rates were therefore GPP rates normalised per chlorophyll. For comparisons of GPP rates determined through 1 h ^{14}C bicarbonate incubations *versus* O_2 evolution over 24 h, ^{14}C values were converted to μmol C L^{-1} h^{-1} and multiplied by a photosynthetic quotient of 1.4 (Laws, 1991). The terms GPP(^{14}C) and GPP(O_2) were used to distinguish between the two methods.

2.4. Bacterial production

Bacterial production was determined every 2 days using ^{14}C-leucine and the micro-centrifuge method of Kirchman (2001). The saturating concentration of ^{14}C-leucine was experimentally determined to be 35 nM (data not shown). For each treatment there were three replicates plus two controls incubated in the dark at 4 °C for 2 h. Samples were killed by adding 100% trichloroacetic acid (TCA) and centrifuged, then rinsed three times to remove excess isotope that was precipitated. For radioactive counts, 1 mL of Ultima Gold scintillation fluid was added to each microcentrifuge tube and measured using a Beckman LS6500 liquid scintillation counter.

Total bacterial abundances were determined using a Becton-Dickinson FACSCalibur flow cytometer fitted with a 488 nm argon laser (Marie et al., 1999; Thomson et al., 2016). Samples were filtered through 50 μm mesh and fixed for 1 h at a final concentration of 0.5% glutaraldehyde. They were then stained for 20 min using a 1:10,000 final dilution of SYBR-Green I (Molecular Probes). Each sample was weighed to ± 0.0001 g before and after analysis to determine the sample volume analysed. Samples were run for 3 min at approximately 35 μL min^{-1} using MilliQ water as sheath fluid. Bacterial concentrations were determined using event counts from bivariate scatter plots of side-scatter (SSC) *versus* SYBR-Green I fluorescence (FL1), and the analysis volume (see also Thomson et al., 2016). PeakFlow Green 2.5 μm beads (Molecular Probes) were added to all samples as an internal fluorescent standard.

Calculations for total bacterial production [μg C L^{-1} h^{-1}] through ^{14}C-leucine incorporation followed that of Smith and Azam (1992). They assumed an intracellular isotope dilution factor of 2, a molar leucine:protein ratio of 0.073, and a carbon:protein ratio of 0.86 (by weight). Cell-specific bacterial productivity [μg C (cell)$^{-1}$ h^{-1}] was calculated through division of total bacterial production by cell abundance. The term "production" was utilised for total bacterial production (μg C L^{-1} h^{-1}), and "productivity" for cell-specific bacterial carbon uptake (μg C cell h^{-1}).

2.5. Additional monitoring of tanks

Particulate organic carbon (POC), dissolved organic carbon (DOC) and macronutrient concentrations were measured every 2 days in the tanks according to the methods of Davidson et al. (2016) and Pearce et al. (2007). Macronutrients were analysed using flow-injection analysis and included nitrate + nitrite (NOx), phosphate and silicate (Davidson et al., 2016). Other measurements in the tanks included HPLC pigment concentrations (Wright et al., 2010) and protistan composition and abundances determined using light and scanning electron microscopy (Davidson et al., 2016). These methods and results are reported elsewhere in detail (Davidson et al., 2016; Thomson et al., 2016). Ratios of Si:N drawdown were examined to determine possible iron limitation of phytoplankton (Westwood et al., 2010; Sugie and Yoshimura, 2016) but were unfortunately too variable due to NOx frequently being below detection limits. As data points for each treatment over time in each experiment were sequential samples from a single tank, all graphs use spline curves to interpolate between data points.

Table 1
Initial conditions in the minicosm tanks for each experiment. Standard deviations are shown where applicable.

	Early-Summer	Mid-Summer	Late-Summer
Chlorophyll *a*, μg L^{-1}	0.38	1.71	2.99
Bacteria, cells ml^{-1}	0.38 × 10^6	1.32 × 10^6	1.10 × 10^6
pH	8.5	8.7	8.4
CO_2, ppm	102	118	232
O_2, μmol L^{-1}	442.0	475.9	391.9
O_2, % saturation	134.4	136.8	110.8
NOx, μM	6.9 ± 1.8	0.15 ± 0.19	3.2 ± 0.5
Phosphate, μM	0.75 ± 0.12	0.21 ± 0.07	0.44 ± 0.08
Silicate, μM	86.9 ± 17.3	67.9 ± 16.9	75.6 ± 10.0
Temperature, °C	2.3	0.3	−0.3
Salinity, psu	33.4	32.6	33.1

3. Results

3.1. Initial conditions for each experiment

For all experiments, the coastal seawater used to fill minicosm tanks had a low CO_2 content (102–232 ppm) and high pH (8.4–8.7, Table 1). Initial CO_2 was lowest in the early-summer experiment. Concentrations slowly increased during the season, but remained well below atmospheric levels (390 ppm atmospheric at the time of experimentation) by late summer. CO_2 was therefore more similar to pre-industrial concentrations than present-day at the start of each experiment. The control treatments (× 0.2 or × 0.5 present-day CO_2) consisted of untreated filtered seawater on Day 0, but were dosed with CO_2 saturated seawater thereafter to compensate for photosynthetic drawn down. Initial chlorophyll in the minicosm tanks ranged from lowest concentrations in the early-summer experiment (0.38 μg L^{-1}), increasing to bloom conditions in the late-summer experiment (2.99 μg L^{-1}, Table 1). Initial bacterial abundance was also lowest in the early-summer experiment (0.38 × 10^6 cells mL^{-1}), with highest initial abundance in the mid-summer experiment (1.32 × 10^6 cells mL^{-1}, Table 1).

Initial concentrations of NOx, phosphate and silicate were highest in the early-summer experiment, lowest in mid-summer, with an increase by late-summer (Table 1). NOx was close to an undetectable concentration (0.15 μM) at the start of the mid-summer experiment, but was initially non-limiting in the other two experiments. Initial silicate concentrations were an order of magnitude higher than NOx concentrations across the season (Table 1). Oxygen concentrations were super-saturated across the season (Table 1). For this reason, oxygen data from the first two days of experimentation were excluded from analyses due to possible out-gassing into minicosm tank headspaces as equilibration occurred. Nutrient concentrations fell within those previously reported off Davis Station, ranging from undetectable concentrations in summer to 25 μM in winter (Gibson, 1998).

Average light intensities for empty tanks at top (incoming light), middle and near-bottom depths corresponded to 393 ± 87, 233 ± 26 and 127 ± 13 μmol m^{-2} s^{-1}, respectively. The average vertical light attenuation (K_d) across all tanks was 1.68 ± 0.19 m^{-1}. This value was similar to that determined in previous minicosm experiments by N. Cadman (personal communication) in water-filled tanks of 1.62 m^{-1} (K_d water). To calculate changes in vertical light attenuation due to increases in chlorophyll concentration during experimentation, the equation of N. Cadman (personal communication) was used;

$$K_d \text{ biomass} = 0.0451157 * \text{chl } a \text{ (mg m}^{-3}\text{)}, \quad \text{m}^{-1}$$

Total light attenuation (K_d total) in the tanks on each day during experimentation was calculated by the addition of K_d water and K_d biomass. Average irradiances (Riley, 1957) calculated from the daily K_d total and a cell circulation depth of 1.14 m (tank depth) ranged from 187 to 296 μmol m^{-2} s^{-1}. Therefore, despite chlorophyll increases, at no point was light limiting to phytoplankton photosynthesis in the tanks given that the maximum intensity for saturation across all tanks and experiments was 54 μmol m^{-2} s^{-1} (see Section 3.4). The daily incoming light dose that tanks received with a light/dark period of 19 h/5 h was 26.9 mol m^{-2} d^{-1}.

3.2. CO_2 during experimentation

There was a clear distinction in CO_2 concentrations among treatments during each experiment, showing that dosing was maintained appropriately (Fig. 1; Thomson et al., 2016). The average CO_2 concentration for the × 6.1 treatment in the early-summer experiment was 2423 ppm. For the mid- and late-summer experiments, average CO_2 concentrations for the × 4 treatments were 1530 and 1711 ppm, respectively. Across all experiments, the CO_2 concentrations in duplicated treatments (× 4.8 in the early-summer experiment or × 3 in subsequent experiments) were always similar. CO_2 concentrations were most variable in the × 6.1 and × 4 treatments across all experiments (Fig. 1). This was likely caused by the decreased buffering ability of seawater at higher CO_2, and the possibility that minicosm tanks were not completely gas tight during some sampling, with strong diffusion gradients facilitating escape. For the early-summer experiment, there was a dip in CO_2 below target concentrations across all treatments between Days 5 and 6 (Fig. 1A). This was caused by CO_2 drawdown due to high rates of photosynthesis and the brief excursion was immediately corrected upon detection (Davidson et al., 2016).

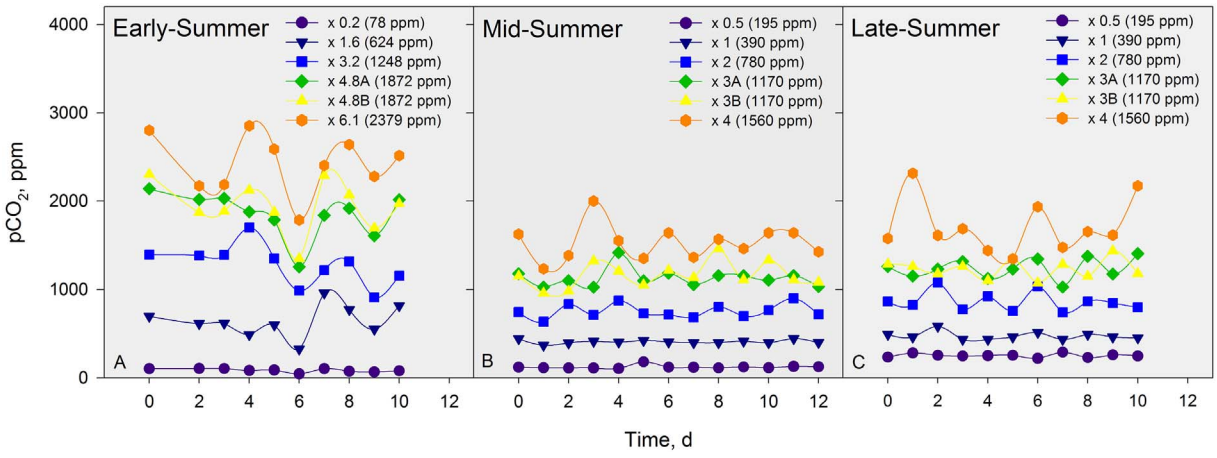

Fig. 1. pCO_2 concentrations (ppm) for each treatment during the early-, mid- and late-summer experiments conducted in minicosm tanks.

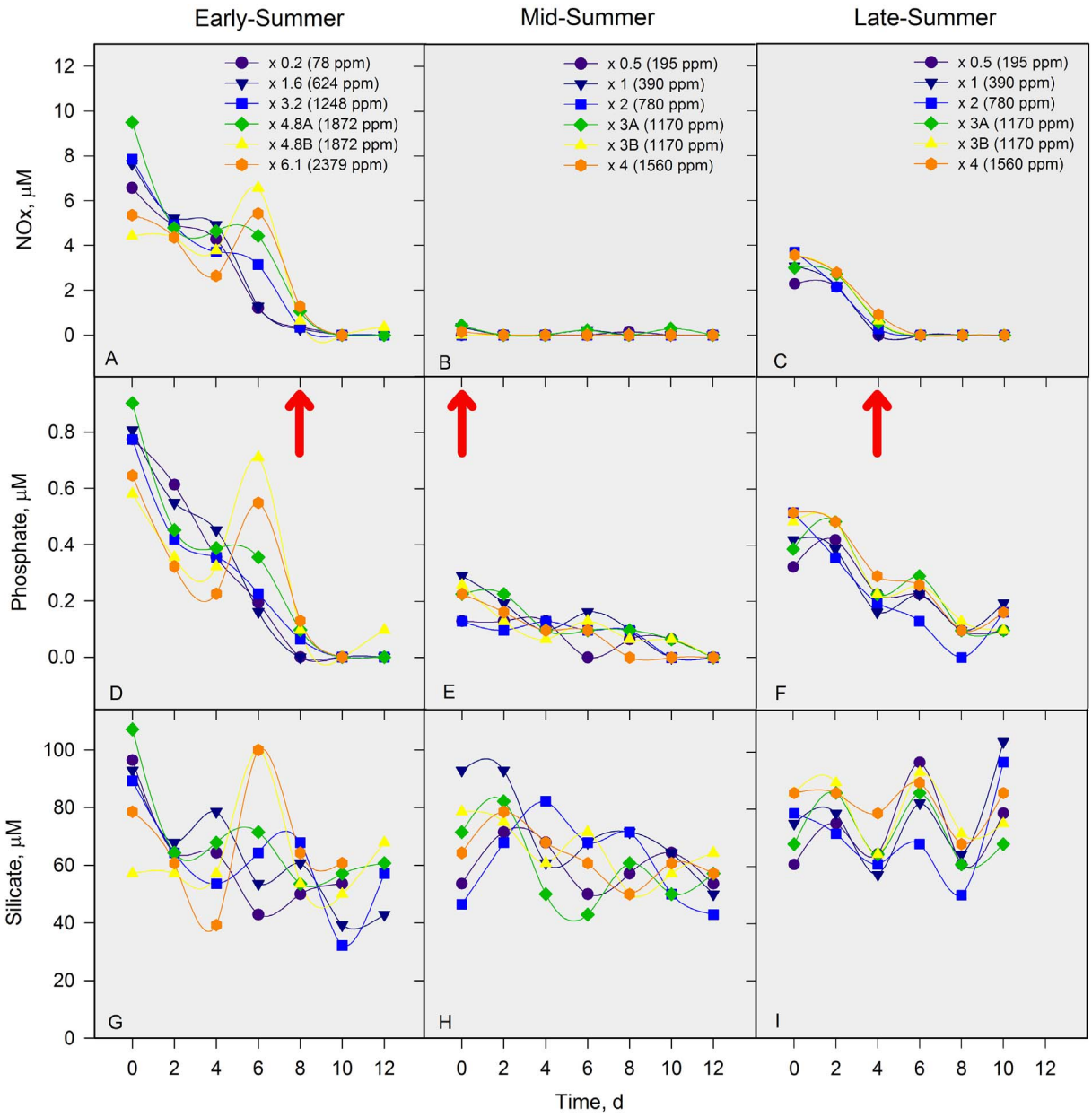

Fig. 2. Dissolved nutrient availability during each experiment. Nitrate + nitrite = NOx. Arrows indicate NOx < 1.5 µM.

3.3. Nutrient availability during experimentation

NOx was drawn down to undetectable concentrations in all experiments, suggesting that this was the main macronutrient controlling growth (Fig. 2A–C; Thomson et al., 2016). For the early-summer experiment, NOx was < 1.5 µM by Day 8. In mid-summer, NOx concentrations were close to undetectable limits at the start of experimentation (see above) and remained so throughout the incubation period. In late-summer, NOx was < 1.5 µM by Day 4. Ratios of N:P averaged 14.2 in the early-summer experiment, close to the Redfield ratio of 16 for phytoplankton (Redfield, 1958). The mid- and late-summer experiments showed strong nitrogen limitation with N:P ratios of 6.2 and 5.0, respectively. Si was never limiting, despite rapid diatom growth in the early-summer experiment (Fig. 2G–I, Davidson et al., 2016).

There were no clear differences in rates of nutrient drawdown (NOx, phosphate or silicate) among CO_2 treatments within each experiment (Fig. 2), despite differences in productivity (see Section 3.4). This may have been due to high variability in macronutrient measurements, as evidenced on Day 0 for each experiment where concentrations should theoretically have been similar across tanks. It is unknown why this variability occurred. There was a sudden increase in nutrient concentrations during the early-summer experiment in the × 4.8B and × 6.1 treatments on Day 6 (Fig. 2A,D,G), probably due to contamination (Davidson et al., 2016).

3.4. Phytoplankton responses to CO_2

Typical photosynthesis-irradiance (P–I) responses to CO_2 are shown in Fig. 3. R^2 values for all modelled P–I curves (n = 114) across all experiments ranged from 0.89 to 0.99, demonstrating significant fits to the data. For the early-summer experiment the range of maximum photosynthetic rates (P_{max}) across all treatments and days was 1.7–5.8 mg C (mg chl a^{-1}) h^{-1} with standard errors ranging from 0.08–0.30. Average photosynthetic efficiencies (α) ranged from 0.042–0.144 mg C (mg chl a)$^{-1}$ h^{-1} (µmol m^{-2} s^{-1})$^{-1}$ with standard errors ranging from 0.0076–0.0089. For the mid-summer experiment, P_{max} ranged from 1.2–2.7 ± 0.041–0.192 mg C (mg chl a^{-1}) h^{-1}

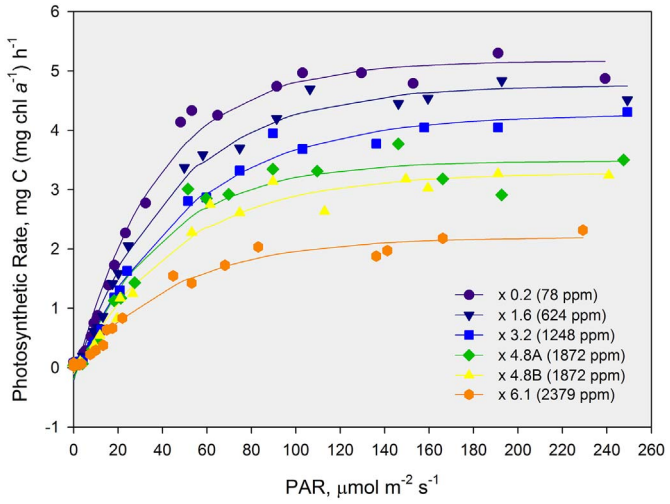
Photosynthetic Rate, mg C (mg chl a-1) h-1
PAR, µmol m-2 s-1
x 0.2 (78 ppm)
x 1.6 (624 ppm)
x 3.2 (1248 ppm)
x 4.8A (1872 ppm)
x 4.8B (1872 ppm)
x 6.1 (2379 ppm)

Fig. 3. Photosynthesis-irradiance (P–I) curves from the early-summer experiment on Day 8. Data points indicate measured data and lines indicate modelled data. PAR = photosynthetically active radiation.

across treatments and days, and α ranged from 0.038–0.086 ± 0.0034–0.017 mg C (mg chl $a)^{-1}$ h^{-1} (µmol m^{-2} $s^{-1})^{-1}$. For the late-summer experiment, P_{max} ranged from 0.5–2.0 ± 0.020–0.062 mg C (mg chl a^{-1}) h^{-1} and α ranged from 0.017–0.052 ± 0.0019–0.0061 mg C (mg chl $a)^{-1}$ h^{-1} (µmol m^{-2} $s^{-1})^{-1}$. Overall, standard errors for both P_{max} and α were one to two orders of magnitude lower than measured values and therefore acceptable.

Elevated CO_2 had a direct negative effect on phytoplankton productivity during all experiments (Figs. 3 and 4). P_{max} generally slowed with elevated CO_2 concentrations (Fig. 4A–C). Similarly, α declined with elevated CO_2 (Figs. 3 and 4D–F). The trend of lowered P_{max} and α under elevated CO_2 did not change throughout experimentation suggesting that there was no adaptation. There was no discernible effect of CO_2 on saturating light intensities (E_k) for any experiment, and values ranged from 22 to 54 µE m^{-2} s^{-1} (Fig. 4G–I). Depressed P_{max} and α under elevated CO_2 coincided with reduced chlorophyll in the early-summer experiment (Fig. 5A, Thomson et al., 2016), whereas no chlorophyll responses were seen in the latter two experiments (Fig. 5B,C, Thomson et al., 2016). There was also a reduction in POC concentrations with elevated CO_2 in the early-summer experiment, but generally no reductions in the latter two experiments except in the × 4 treatments (Fig. 5D–F). There were no clear relationships between concentrations of CO_2 and DOC in any experiment (Fig. 5G–I), with high variability in DOC measurements.

Reduced productivity (P_{max}) under elevated CO_2 caused a clear reduction in total phytoplankton production [GPP(^{14}C)] in the minicosm tanks throughout the summer season (Fig. 6A–C). Every experiment showed that GPP(^{14}C) rates declined with elevated CO_2. In general, rates of GPP(^{14}C) were similar at CO_2 concentrations < × 2 (780 ppm), but noticeably decreased at concentrations > × 2. Highest CO_2 treatments (× 6.1 or × 4) caused a 27–65% reduction in GPP(^{14}C) compared to controls (× 0.2 or × 0.5) across all experiments. Strongest responses to CO_2 occurred in the early-summer experiment (Fig. 6A).

GPP(^{14}C) rates were fastest during the early-summer experiment, ranging from 0.6 to 26.4 mg C L^{-1} h^{-1} (Fig. 6A). Slowest GPP(^{14}C) rates occurred in the mid-summer experiment, ranging from 1.5 to 3.0 mg C L^{-1} h^{-1} (Fig. 6B). For the late-summer experiment, GPP(^{14}C) measurements ranged from 1.4 to 8.7 mg C L^{-1} h^{-1}. However, rates were slow in the late-summer experiment given the high biomass of phytoplankton in the tanks (Table 1, Fig. 6C), suggesting that the population was becoming senescent. This was supported by lowest P_{max} and α values (Fig. 4C,F). In the early-summer experiment, rates of GPP (^{14}C) generally started to decline on Day 8, and in the late-summer experiment on Day 4 (Fig. 6A,C). Largest reductions occurred in low CO_2 treatments. There were no marked changes in GPP(^{14}C) rates during the mid-summer experiment (Fig. 6B).

3.5. Bacterial responses to CO_2

Elevated CO_2 also had a direct negative effect on bacterial productivity during experimentation (Fig. 7), with clear decreases in cell-specific carbon uptake with increasing CO_2 across all experiments. Similar to phytoplankton, this response to elevated CO_2 was consistent throughout the season despite changing environmental conditions. Furthermore, the most obvious CO_2-induced decreases in productivity occurred at concentrations > × 2 (780 ppm). Fastest rates of cell-specific bacterial productivity were observed in the early-summer experiment (Fig. 7A), despite lowest DOC concentrations during this time (Fig. 5G).

Decreased cell-specific bacterial productivity in elevated CO_2 treatments did not cause a decrease in total bacterial production. Rather, rates of production were faster for elevated CO_2 treatments (> × 2) compared to lower concentrations, over the first two days of experimentation (Fig. 8A–C). This was also observed in bacterial abundance measurements with higher concentrations under elevated CO_2 over Days 0–4 (Fig. 8D–F, Thomson et al., 2016). Thus, whilst carbon uptake was impaired under elevated CO_2 concentrations (Fig. 7), this was overcompensated for by higher numbers of bacteria in the same treatments. Increased bacterial production and abundance with elevated CO_2 coincided with lower abundances of heterotrophic nanoflagellates (Fig. 8G–I, Thomson et al., 2016). There was a significant linear correlation between bacterial production and abundance measurements [production = $(6.94 \times 10^{-7}) \times$ abundance + 0.7179, n = 114, df = 112, r^2 = 0.694, two-tailed test $P < 0.001$], but no effect of CO_2 on the relationship.

Rates of bacterial production were slowest in the early-summer experiment and ranged from 0.02 to 1.9 µg C L^{-1} h^{-1} (Fig. 8A). For the mid- and late-summer experiments, production ranged from 0.9 to 3.0 and 0.7 to 2.1 µg C L^{-1} h^{-1}, respectively (Fig. 8B,C). For all experiments, rates of bacterial production were over three orders of magnitude slower than GPP(^{14}C) rates (Figs. 6A–C and 8A–C). Thus, bacterial respiration did not substantially influence observed rates of NCP.

3.6. Net community production (NCP)

For the early- and late-summer experiments, NCP showed the same response to CO_2 as GPP(^{14}C), with slowed rates under elevated concentrations (Fig. 9A,C). In the early-summer experiment, CO_2 effects on NCP were only evident until Day 8, and in the late-summer experiment until Day 4. Thereafter, NCP was similar among CO_2 treatments and declined. The mid-summer experiment differed in that NCP was never affected by CO_2 (Fig. 9B). For this experiment, NCP rates were mostly negative with only some positive values towards the end of the experiment. This indicated that rates of respiration were faster than photosynthesis, resulting in a net heterotrophic community. Accordingly, ratios of photosynthesis to respiration (P:R) were generally < 1 in the mid-summer experiment (Fig. 10B). For the early- and late-summer experiments, changes in CO_2 effects on NCP coincided with a switch in P:R ratios (Fig. 10A,C). Initially, P:R values increased with time indicating that the systems were increasingly autotrophic. Values then decreased indicating a change from autotrophy to heterotrophy. The onset of declining ratios of P:R and the disappearance of CO_2-induced effects on NCP coincided with NOx concentrations < 1.5 µM (indicated by arrows, Figs. 10A–C, 9A–C, see also Fig. 2A–C).

The effect of CO_2 on respiration rates was less clear than for NCP (Fig. 9D–F). For the early-summer experiment there was a decrease in respiration rates with elevated CO_2 (Fig. 9D), similar to NCP. During

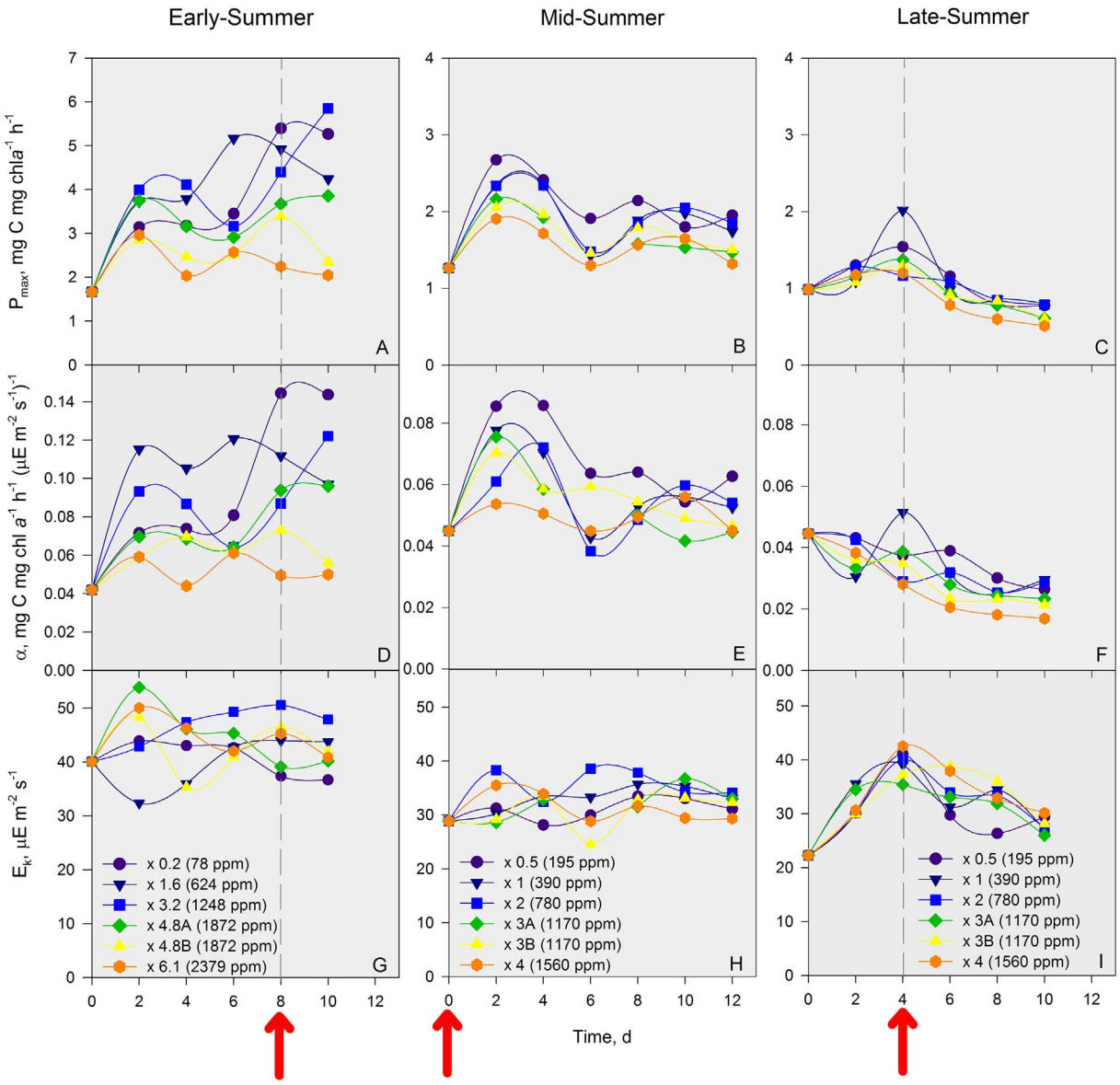

Fig. 4. Photosynthetic parameters derived from photosynthesis *versus* irradiance (P–I) curves for each CO_2 treatment. P_{max} = maximum photosynthetic rate, α = photosynthetic efficiency, E_k = light intensity for saturation of photosynthesis. Arrows indicate NOx < 1.5 µM.

late-summer there was no obvious effect of elevated CO_2 on respiration (Fig. 9F), however this may partially have been due to low values which increased variability. For the mid-summer experiment rates of respiration were similar between CO_2 treatments (Fig. 9E).

GPP(O_2) rates generally showed the same trends as respiration rates across all experiments (Fig. 9G–I). GPP(O_2) rates were fastest in the early-summer experiment (Fig. 9G) with a range of 0.2 to 3.2 µmol O_2 L^{-1} h^{-1} (data Days 0–2 excluded). Slowest rates were in the mid-summer experiment, ranging from 0.05 to 0.47 µmol O_2 L^{-1} h^{-1} (Fig. 9H, data Days 0–2 excluded). For the late-summer experiment, values ranged from 0.4 to 1.4 µmol O_2 L^{-1} h^{-1} (Fig. 9I, data Days 0–2 excluded). Similar to GPP(^{14}C), rates of GPP(O_2) were slow in the late-summer experiment given the high biomass of phytoplankton in the tanks, again suggesting that the population was becoming senescent.

Comparisons of GPP rates calculated from short term (1 h) $NaH^{14}CO_3$ uptake [GPP(^{14}C)] *versus* long term (24 h) oxygen changes [GPP(O_2)] showed a generally linear relationship for the early- and late-summer experiments (Fig. 11A,C). There was no relationship for the mid-summer experiment (Fig. 11B), which was expected given that the population was heterotrophic. In the late-summer experiment, GPP (O_2) values were clearly higher than GPP(^{14}C) values (Fig. 11C), whereas the data approached a 1:1 relationship in the early-summer experiment (Fig. 11A). Across all experiments, there was no effect of elevated CO_2 on the relationship between GPP(^{14}C) and GPP(O_2) (Fig. 11).

4. Discussion

4.1. Phytoplankton

Despite differing microbial communities (Thomson et al., 2016) and NOx availabilities during austral summer in Antarctica, there were consistent phytoplankton and bacterial responses to OA across the season (Table 2). The clearest impact of OA in our study was that rates of GPP(^{14}C) decreased with elevated CO_2 (Fig. 6). Reduced GPP(^{14}C) was caused through decreased maximum photosynthetic rates (P_{max}). There was also strong evidence that α was decreased with elevated CO_2, however the minicosm tanks were always light-saturated so that α was not included in GPP(^{14}C) calculations. Significant reductions in GPP (^{14}C) were generally seen at CO_2 concentrations > × 2 present-day

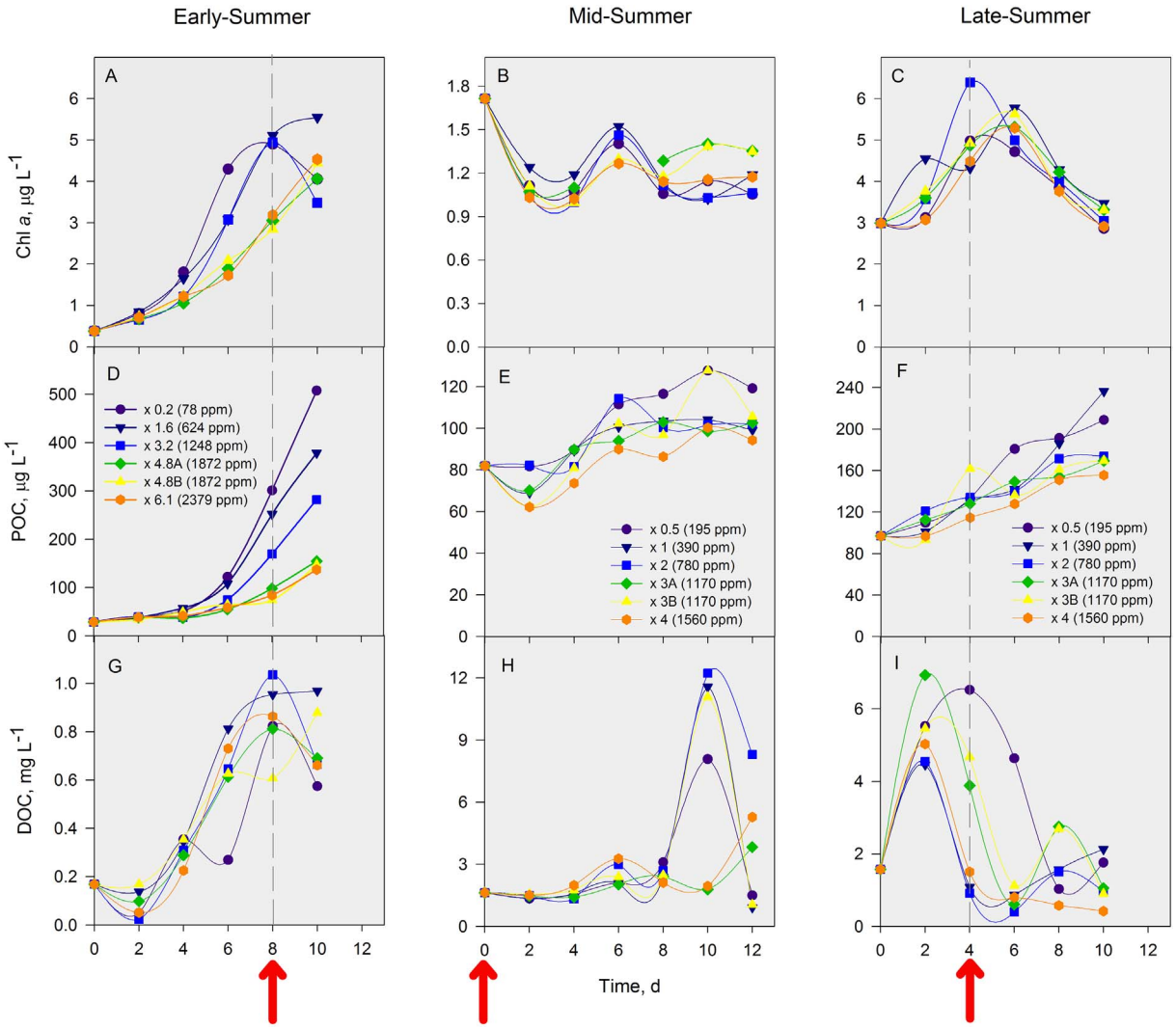

Fig. 5. Changes in chlorophyll *a* (Chl *a*), particulate organic carbon (POC) and dissolved organic carbon (DOC) with time for each CO_2 treatment. Arrows indicate NOx < 1.5 µM.

(*i.e.* > 780 ppm, Fig. 6). The general lack of responses at lower concentrations is perhaps unsurprising given the large *in situ* fluctuations of CO_2 that occur in Antarctic coastal waters (Gibson and Trull, 1999; Roden et al., 2013). The finding suggests that Antarctic microbial communities may initially show some resilience to OA as conditions intensify. CO_2 treatments were generally not replicated within each experiment (aside from one treatment), but the consistent response of three experiments across the season suggested that the data adequately represented the effects of CO_2 on the microbial community, with the results unlikely to be due to random variation.

The results of our study were the opposite of mesocosm studies in polar (Brussaard et al., 2013; Engel et al., 2013; Piontek et al., 2013) and temperate waters (Riebesell et al., 2007; Egge et al., 2009; de Kluijver et al., 2010), where elevated CO_2 caused an increase rather

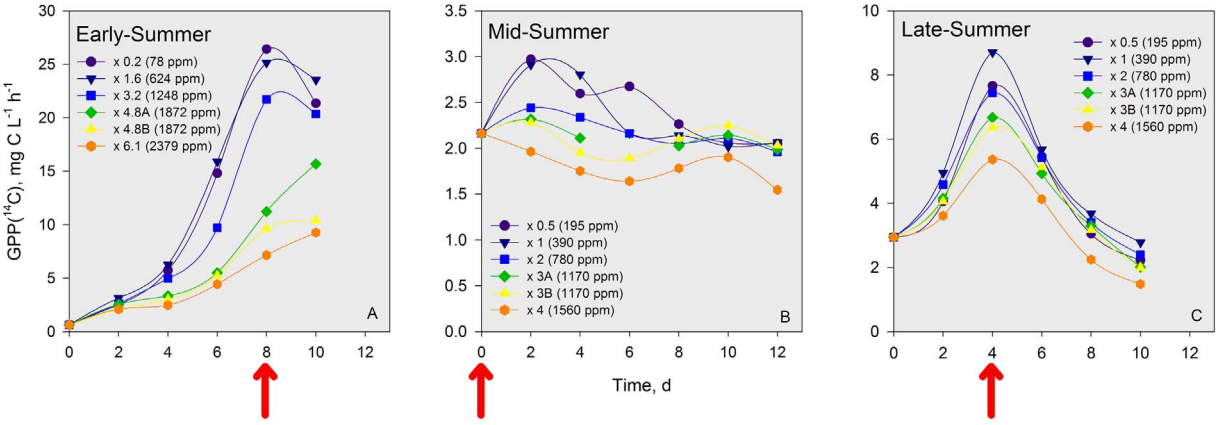

Fig. 6. Changes in rates of gross primary production (GPP(^{14}C)) with time for each CO_2 treatment, as determined using $NaH^{14}CO_3$. Arrows indicate NOx < 1.5 µM.

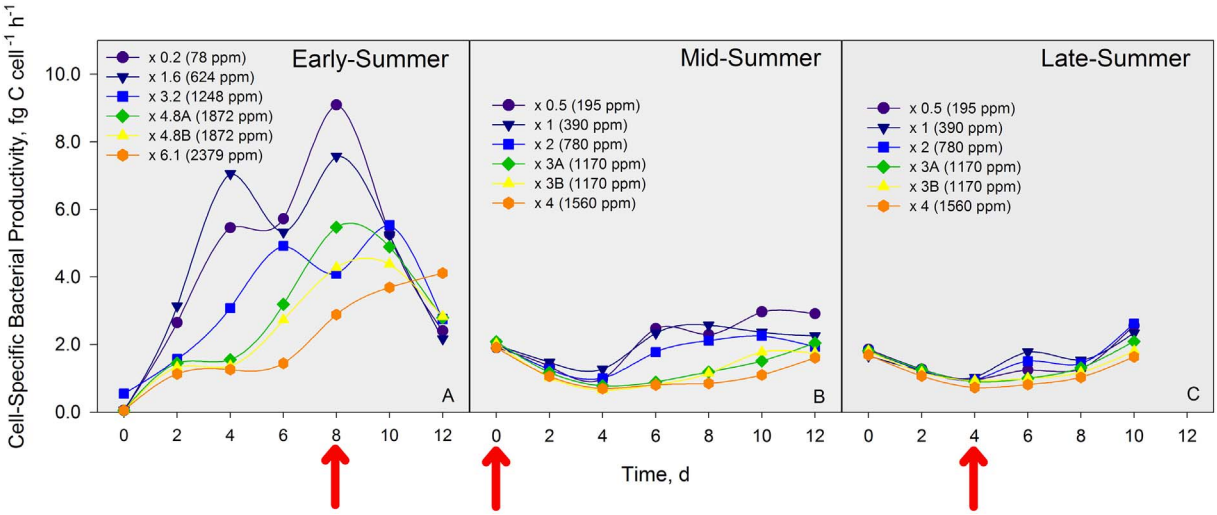

Fig. 7. Changes in cell-specific bacterial productivity (carbon uptake per cell) with time for each CO_2 treatment, as determined using ^{14}C-leucine. Arrows indicate NOx < 1.5 μM.

than decrease in production. In our study CO_2 target concentrations were maintained throughout experimentation, whereas the mesocosm experiments had CO_2 doses administered at the start of experimentation, with subsequent drawn down as time progressed. This difference in approach meant that the total carbon dose over a whole experiment was considerably higher for a given CO_2 treatment in our study and is a potential reason for different outcomes. However, in other studies where CO_2 concentrations were maintained throughout

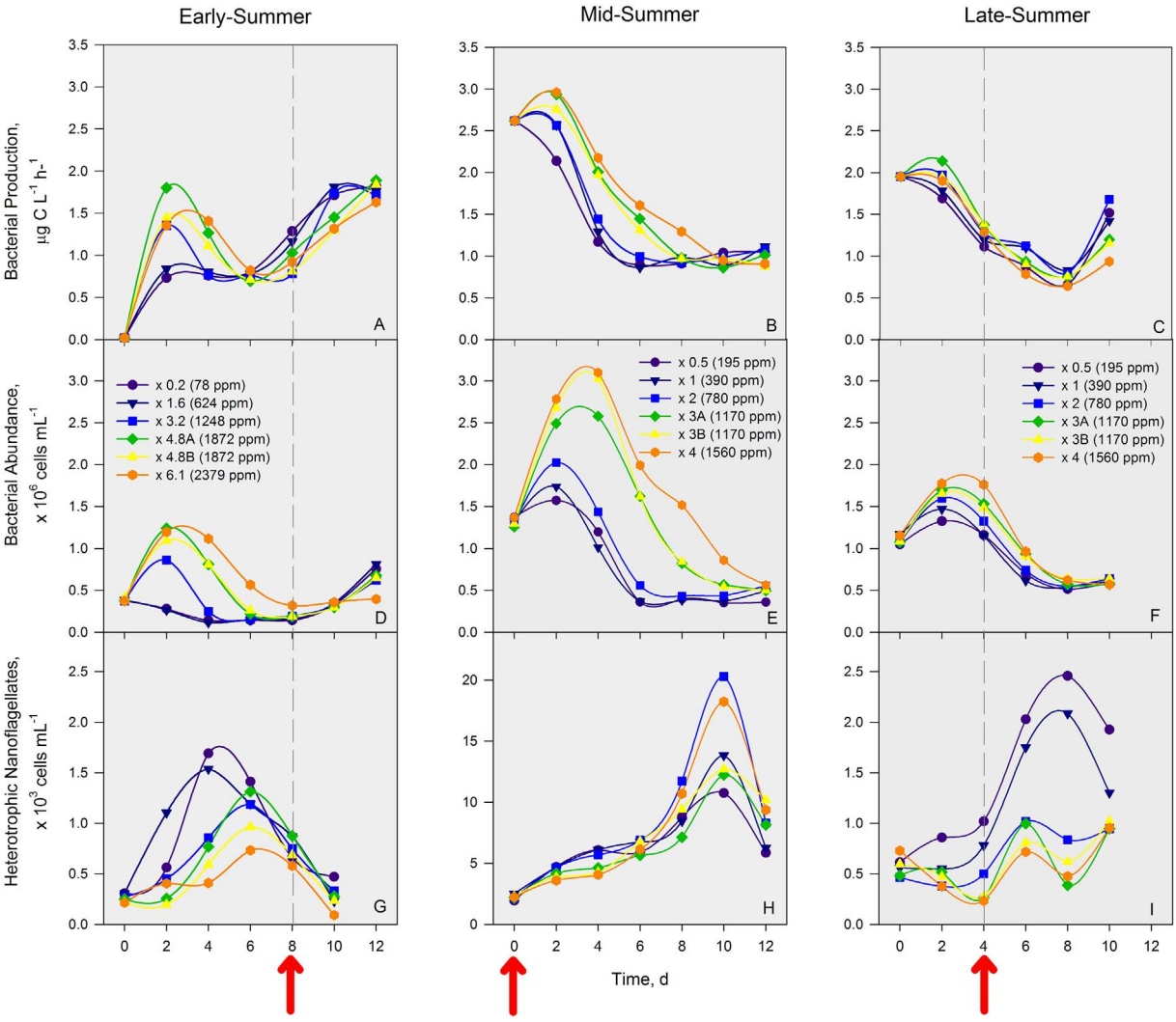

Fig. 8. Changes in bacterial production, bacterial abundances and heterotrophic nanoflagellate abundances with time for each CO_2 treatment. Arrows indicate NOx < 1.5 μM.

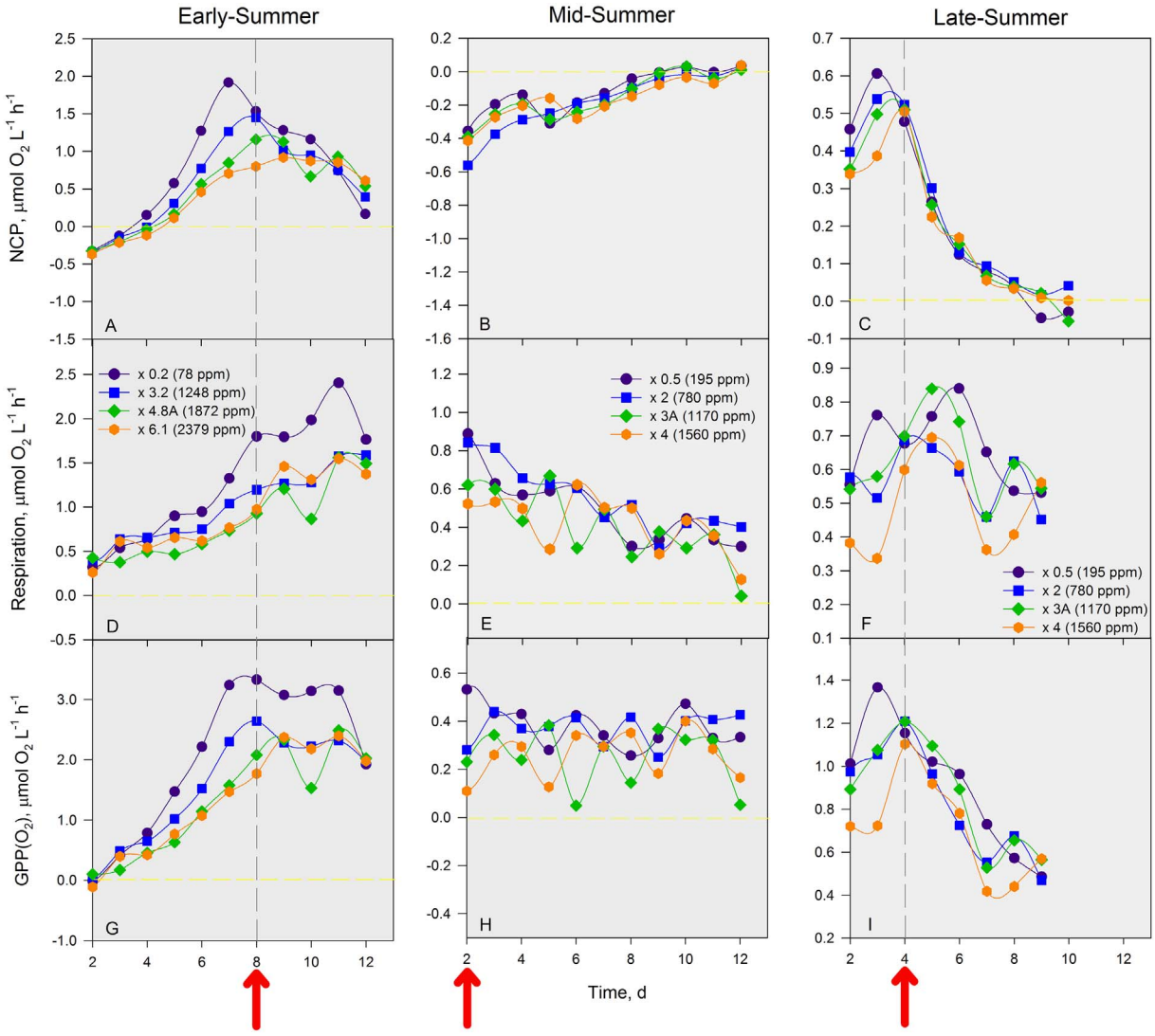

Fig. 9. Rates of net community production (NCP), respiration, and gross primary production ($GPP(O_2)$) calculated from oxygen changes in minicosm tanks for each CO_2 treatment. Respiration rates are plotted as positive rather than negative values for comparisons with NCP. Arrows indicate NOx < 1.5 µM. Data from Days 0–2 excluded due to the possibility that oxygen had not yet equilibrated with overlying headspaces in the minicosm tanks.

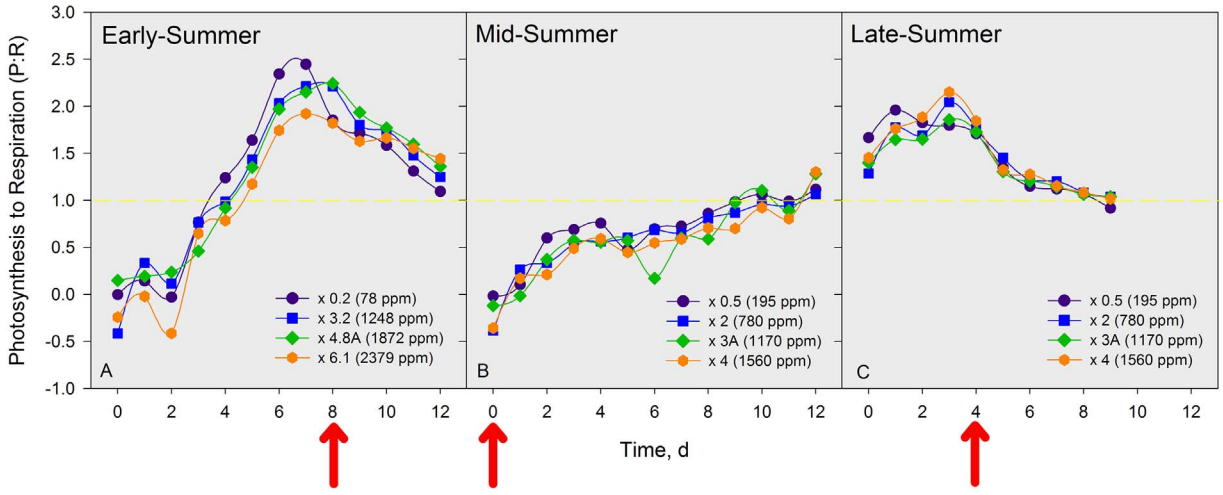

Fig. 10. Changes in photosynthesis to respiration ratios (P:R) with time for each CO_2 treatment. Arrows indicate NOx < 1.5 µM. Data from Days 0–2 excluded due to the possibility that oxygen had not yet equilibrated with overlying headspaces in the minicosm tanks.

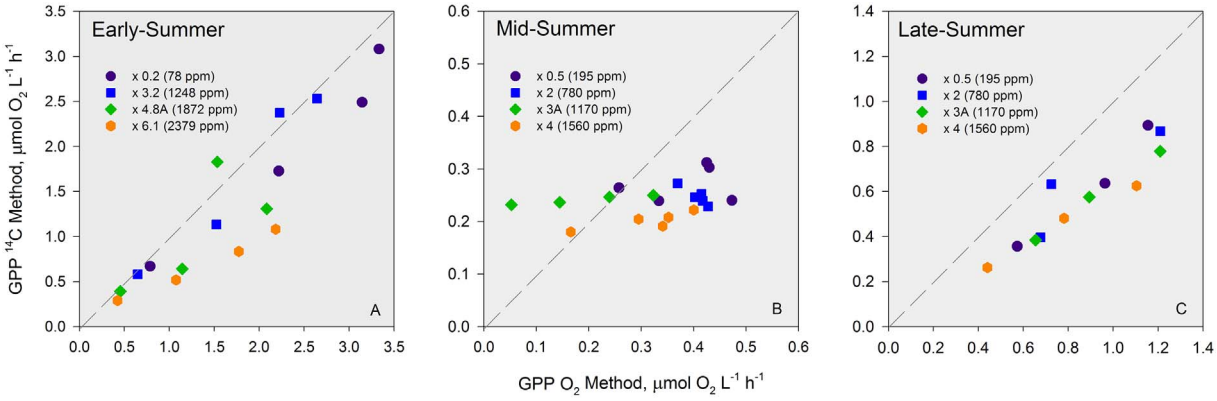

Fig. 11. Comparison of gross primary production (GPP) rates determined using oxygen ($GPPO_2$) and $NaH^{14}CO_3$ ($GPP^{14}C$) methods. Data from Days 0–2 excluded due to the possibility that oxygen had not yet equilibrated with overlying headspaces in the minicosm tanks. Dashed lines indicate a 1:1 relationship.

experimentation (similar to our study), responses were also different (Tortell et al., 2008; Hoppe et al., 2013; Young et al., 2015). Young et al. (2015) incubated Antarctic phytoplankton over 2 to 3 weeks but found no significant changes in production or growth with elevated CO_2. It should be noted though that the highest CO_2 treatment (800 ppm) in these experiments may not have been sufficient to induce negative production or growth, as evidenced by our experiments where changes occurred at concentrations > 780 ppm (see above). Tortell et al. (2008) and Hoppe et al. (2013) did find a CO_2 effect at 800 ppm, with increased rather than decreased production. However, no response was found under iron limitation (Hoppe et al., 2013).

The absence of an acclimation period for microbes to adjust to

Table 2
Summary of the characteristics of each minicosm experiment conducted during austral summer in Antarctica, and the associated responses to elevated CO_2. Shaded boxes indicate consistent responses across the season. NOx = nitrate + nitrite, PP = primary productivity, GPP = gross primary production, BP = bacterial productivity or bacterial production, NCP = net community production, POC = particulate organic carbon, DOC = dissolved organic carbon.

	Early-Summer	Mid-Summer	Late-Summer
INITIAL	Low chlorophyll	Intermediate chlorophyll	High chlorophyll
	Low bacteria	High bacteria	Intermediate bacteria
	High NOx	No NOx	Intermediate NOx
	Autotrophic	Heterotrophic	Autotrophic
RATES	Chlorophyll-specific PP fast	Chlorophyll-specific PP slow	Chlorophyll-specific PP slow
	Total GPP fast	Total GPP slow	Total GPP intermediate
	Cell-specific BP fast	Cell-specific BP slow	Cell-specific BP slow
	Total BP slow	Total BP fast	Total BP intermediate
	NCP fast	NCP slow	NCP intermediate
RESPONSES TO CO_2	↓ Chlorophyll-specific PP	↓ Chlorophyll-specific PP	↓ Chlorophyll-specific PP
	↓ Total GPP	↓ Total GPP	↓ Total GPP
	↓ Chlorophyll	No change chlorophyll	No change chlorophyll
	↓ POC	No change POC	no change POC
	DOC variable	DOC variable	DOC variable
	↓ Cell-specific BP	↓ Cell-specific BP	↓ Cell-specific BP
	↑ Total	↑ Total BP	↑ Total BP
	↓ Heterotrophic nanoflagellates	↓ Heterotrophic nanoflagellates	↓ Heterotrophic nanoflagellates
	↓ NCP	No change NCP	↓ NCP
	↓ Respiration	No change respiration	No change respiration

elevated CO_2 in our experiments may also have caused differing responses to other studies (Davidson et al., 2016; Bell and Gonzalez, 2011). The minicosm tanks were filled with water from offshore and CO_2 added half a day later. For dosing, CO_2-saturated seawater was added over 2 h to bring the various treatments up to target concentrations. A sudden increase in CO_2 over 2 h rather than a slower increase over days may have selected for species with high phenotypic plasticity rather than species with fastest rates of photosynthesis and growth (Schaum et al., 2013). Further OA work in the minicosms where the Antarctic microbial population was incubated for 18 days (similar to Young et al., 2015) yielded similar responses to our study (Deppeler et al., in review). In that experiment, cells were incrementally acclimated to CO_2 over 5 days. Long acclimation times allowing a large number of cellular generations are preferable for OA studies (Lohbeck et al., 2012).

One of the main phytoplankton cellular functions that was expected to be affected by increased CO_2 was that of carbon concentrating mechanisms (CCMs; Beardall et al., 1982; Beardall et al., 1991; Giordano et al., 2005; Young and Beardall, 2005; Raven et al., 2012; Mackey et al., 2015; Young et al., 2015). The down-regulation of energetically costly CCMs with CO_2 has been shown to increase production and growth (Mackey et al., 2015), though this is not always the case in Antarctic waters where low temperatures lead to reduced energy requirements for Rubisco saturation (Kranz et al., 2015; Young et al., 2015). It is unknown how CCMs were affected in our experiments (not measured), however production decreased with CO_2 rather than to increase or remain unchanged. It is possible that light intensities in the minicosm tanks were too high in our experiments (Gao et al., 2012). The down-regulation of CCMs under elevated CO_2 removes a buffer against excess energy given that CCMs normally provide an energy sink (Li and Campbell, 2013; Trimborn et al., 2017). The down-regulation of CCMS with elevated CO_2 may therefore increase light stress due to excess energy. Metabolic costs associated with photoprotection and repair may subsequently increase with CO_2 (Li and Campbell, 2013; Hoppe et al., 2015; Trimborn et al., 2017), leading to reduced production and growth. The range of light intensities that phytoplankton were exposed to as they circulated in our minicosm tanks was 127 to 393 μmol m^{-2} s^{-1} (bottom to top), with a daily incoming light dose of 26.9 mol m^{-2} d^{-1}. The daily incoming light dose was 30% less than calculated for 5 m depth on a clear day at the site where water was extracted for our experiments. It should therefore have been appropriate. However, circulation rates within the tanks were rapid (< 5 min) so that cells were often exposed to high light intensities at the surface.

Decreased primary production with elevated CO_2 may also have been related to reduced iron bioavailability (Shi et al., 2010; Hoppe et al., 2013; Sugie et al., 2013). This trace metal is the main limiting nutrient in Antarctic waters (Blain et al., 2007). To prevent limitation in our minicosm tanks we added 5 nM Na[Fe(EDTA)].$3H_20$ at the start of experimentation. However, it is unclear as to whether the iron was bioavailable due to the complexities of iron biogeochemistry (Hassler and Schoemann, 2009). Mesoscale dosing studies in the Southern Ocean have previously shown that iron addition to surface waters stimulates the growth of large diatoms (Boyd et al., 2000; Gervais et al., 2002; Coale et al., 2004). In the early-summer experiment there was rapid growth of large diatoms (> 20 μm) under low CO_2 (Davidson et al., 2016) suggesting that there was sufficient *in situ* iron for this to occur. In contrast, under elevated CO_2 there was significant growth of small rather than large species, including nanoflagellates and small (5 μm) diatoms (Davidson et al., 2016; Thomson et al., 2016). A similar result was found in the Arctic where elevated CO_2 stimulated the growth of pico- and nano-flagellates (Brussaard et al., 2013; Riebesell et al., 2013; Schulz et al., 2013). Small cells have higher surface area to volume ratios so that the efficiency of iron uptake increases (Sunda and Huntsman, 1997; Finkel et al., 2010). If iron bioavailability was reduced under elevated CO_2, smaller cells may have outcompeted larger cells leading to reduced productivity and growth (*e.g.* Peloquin et al., 2010; Boyd et al., 2012). It was intended that Si: N drawdown ratios would be used in our experiments to assess iron limitation (Westwood et al., 2010; Sugie and Yoshimura, 2016), however NO_X was frequently below detection limits. To clarify the role of iron bioavailability in future OA studies, ratios of ferredoxin:flavodoxin proteins could be examined (Erdner et al., 1999), combined with iron-spiking studies and active chlorophyll fluorescence measurements (Hoppe et al., 2013).

The effect of elevated CO_2 on chlorophyll *a* and POC measurements was variable across the summer season, despite consistent reductions in GPP(^{14}C) (Table 2, Fig. 5). Decreased chlorophyll *a* and POC concentrations with elevated CO_2 were only seen in the early-summer experiment when the magnitude of GPP(^{14}C) responses was greatest and NOx was initially non-limiting (Fig. 6). Fast production rates allowed large increases in chlorophyll and POC. For the mid- and late-summer experiments, CO_2 effects on chlorophyll and POC were unclear. GPP(^{14}C) rates were slower in these experiments due to NOx limitation, and the ^{14}C technique may have been more sensitive than chlorophyll or POC measurements in detecting CO_2 effects. Grazing by microzooplankton (Pearce et al., 2010) and viral attack on cells (Brussaard et al., 2013) may also have influenced the net balance of chlorophyll and POC concentrations. Furthermore, shifts in phytoplankton community structure (Davidson et al., 2016) may have confounded chlorophyll responses through potential changes in chlorophyll to carbon ratios (Kruskopf and Flynn, 2006). POC concentrations may also have been influenced by non-phytoplankton cells, particularly in the mid-summer experiment which was heterotrophic. Overall, the factors that influenced chlorophyll and POC concentrations in our minicosm tanks were unclear.

4.2. Bacteria

The response of bacteria to CO_2 was similar to phytoplankton in that cell-specific productivity was reduced in elevated treatments (Fig. 7). Again, this response was consistent for all experiments across the season (Table 2), though the extent of response was significantly lower for the mid- and late-summer experiments compared to the early-summer experiment when nutrients were abundant and the range of CO_2 concentrations greater. The result of reduced bacterial productivity under elevated CO_2 was unexpected and may suggest direct physiological effects on cellular processes. It has long been known that decreased pH affects the ionisation state of amino acids (Tipton and Dixon, 1979). This causes the denaturing of protein chains and alters rates of enzyme-based reactions and/or protein recognition. Decreased pH may also influence proton pumps within cell membranes and mitochondria, affecting transfer of nutrients and metabolites, and the production of energy (Efremov et al., 2010). Similar to phytoplankton, the main decreases in bacterial productivity occurred at CO_2 concentrations > 780 ppm (× 2 present-day).

Decreases in cell-specific productivity of bacteria under elevated CO_2 did not cause coincident decreases in total bacterial production. Rather, rates of total production increased under elevated CO_2 over the first 2 days of experimentation. Similarly, bacterial abundances were higher under elevated CO_2 over the first 4 days (Thomson et al., 2016). The same results occurred across the season (Table 2) and initially seemed contradictory when considering bacteria in isolation from the rest of the microbial loop. However, in the same experiments, Thomson et al. (2016) showed that elevated CO_2 caused decreased growth of heterotrophic nanoflagellates (Table 2, Fig. 8G–I). Increased bacterial production and abundance under elevated CO_2 were therefore likely the result of reduced grazing pressure. As such, the effect of CO_2 on top-down factors had a larger control on bacterial production and population balance than bottom-up effects of the physiological state of the cells. This interaction between various components of the microbial loop demonstrates the importance of community-level studies to determine the impacts of OA. Interestingly, Caron and Hutchins (2013)

showed that elevated CO_2 reduced the motility of grazers because it affected their flagella function. This may partly explain the lack of heterotrophic nanoflagellates in our experiments.

Relationships between bacteria and DOC availability were unable to be established in our experiments due to high variability of DOC concentrations (Table 2, Fig. 5). Previous studies have shown that variability is common due to fast turnover rates as well as the occurrence of DOC in different forms (Scott et al., 2000; Kirchman et al., 1991). DOC is known to provide an important carbon source for bacteria and some studies have reported promotion of bacterial production with elevated CO_2 due to increased DOC concentrations. This was enabled through enhanced phytoplankton production (Grossart et al., 2006; Thingstad et al., 2008; Engel et al., 2013) and increased carbon consumption relative to other nutrients by phytoplankton (Toggweiler, 1993; Riebesell et al., 2007; Bellerby et al., 2008). The excess carbon was then exuded passively or actively as DOC, promoting bacteria or accumulating to form aggregations such as transparent exopolymer particles (Fogg, 1966; Alldredge et al., 1995; Engel, 2002; Kim et al., 2011). In our study, it was likely that changes in DOC did not play a major role in bacterial dynamics given that phytoplankton productivity was reduced rather than enhanced with elevated CO_2. It was therefore likely that less DOC was produced under elevated CO_2, providing less substrate for bacterial growth.

For elevated CO_2 treatments, it may be concluded that increased carbon remained in the DIC pool rather than being channelled into the microbial loop in our experiments. Both phytoplankton and bacterial productivity were reduced due to impaired carbon uptake. This differs from the EPOCA mesocosm experiment in the Arctic where additional carbon was incorporated into the microbial loop. However, in their experiment it was thought that a proportion of carbon was later shunted from the particulate organic pool to the dissolved organic pool due to viral-induced cell lysis (Brussaard et al., 2013; Engel et al., 2013). Further investigation on carbon flow in our minicosm tanks could be undertaken using ^{13}C labeling studies similar to that conducted by de Kluijver et al. (2010).

4.3. Net community production

^{14}C-based assays of phytoplankton and bacteria were conducted over timescales of hours, while NCP integrated the effect of elevated CO_2 over 24 h. NCP therefore provided insight into the fate of carbon once it had been initially fixed, describing the net metabolism of the system (Tanaka et al., 2013). NCP included influences from phytoplankton, bacteria, and all other heterotrophs < 200 μm in the tanks which affected oxygen measurements. NCP responses to elevated CO_2 varied both within and among experiments (Table 2, Fig. 9), driven by NOx availability. There were clear reductions in NCP with elevated CO_2 when NOx was available. When concentrations fell below 1.5 μM there was no longer a CO_2 effect. The occurrence of NOx limitation both within experiments and over the season essentially meant that we conducted a multiple-stressor study, thus providing an interesting insight into the modification of CO_2 responses by another parameter (Boyd, 2011).

When NOx was available in the early- and late-summer experiments, positive P:R ratios indicated that the systems were autotrophic. At these times, NCP was dominated by phytoplankton and reductions in photosynthesis with elevated CO_2 were therefore reflected in NCP measurements. The transition to a decline in NCP and P:R once NOx fell below 1.5 μM was due to either increased respiration from heterotrophs, decreased GPP, or a combination of both. It was demonstrated that bacteria would not have significantly contributed to NCP given that their production rates were negligible compared to phytoplankton. Any changes in respiration were therefore likely due to microzooplankton and/or heterotrophic nanoflagellates, as well as phytoplankton. Respiration measurements were unclear (Fig. 9D–F). However, linear relationships between GPP(O_2) and GPP(^{14}C) in the early- and late-summer experiments suggested that the balance of these systems was driven by photosynthesis, even when NOx was limiting (Fig. 11A,C). If respiration processes had been significant there would have been no agreement between 1 h [GPP(^{14}C)] and 24 h [GPP(O_2)] gross production calculations, as seen in the mid-summer experiment when heterotrophy dominated (Figs. 9B, 11B). Thus, reductions in NCP and P:R with NOx limitation were driven by reduced GPP (Fig. 6A,C) rather than increased respiration (Fig. 9D,F). Largest NOx-induced decreases in GPP occurred in low CO_2 treatments, with rates therefore becoming more similar to elevated CO_2 treatments (Fig. 6A,C).

Reduced NCP by either elevated CO_2 or NOx limitation in our experiments has implications for future ocean conditions. Antarctic waters currently absorb up to 12% of anthropogenic CO_2 emissions through physical and biological processes (Ducklow et al., 2001; DeVries, 2014). As OA intensifies, the efficiency of the biological pump may decrease due to reduced carbon uptake by phytoplankton, thus forming a positive feedback to climate change. Antarctic waters may potentially also experience strengthened stratification with climate change due to increased surface temperatures (Matear and Hirst, 1999), though this may be offset in some regions through increased westerly winds associated with the Southern Annular Mode (Sallée et al., 2010). In areas with strengthened stratification, there may be reduced fluxes of nutrients such as NOx to surface waters, also causing decreased production (Constable et al., 2014; Petrou et al., 2016). Finally, reduced production with OA or NOx limitation may have implications for the Antarctic marine food web, directly influencing krill and zooplankton populations (Nicol et al., 2010), and subsequently higher trophic levels. Not only may elevated CO_2 cause a decrease in primary and net production and therefore food availability, it may also cause a shift to smaller species < 5 μm (Davidson et al., 2016). Krill are inefficient at grazing cells < 10 μm (Boyd et al., 1984; Kawaguchi et al., 1999) and may therefore be at particular risk.

4.4. Conclusions

OA may affect the marine microbial loop through the interplay of bottom-up and top-down controls. In our Antarctic minicosm experiments, CO_2 concentrations > × 2 (780 ppm) decreased both phytoplankton and bacterial productivity. CO_2-induced decreases in phytoplankton productivity (P_{max}, mg C mg chl a^{-1} h^{-1}) clearly lead to reduced primary production (GPP^{14}C, mg C L^{-1} h^{-1}) in all experiments across the summer season. For bacteria, elevated CO_2 decreased cell-specific productivity yet overall production increased. This appeared to be due to the release of grazing pressure by heterotrophic nanoflagellates (Thomson et al., 2016). Net community production generally reflected GPP(^{14}C) under NOx replete conditions and was therefore influenced by CO_2 at these times. Under NOx limitation, CO_2 effects were suppressed and communities switched from net autotrophy to heterotrophy with a decline in NCP. Overall, whilst OA may reduce productivity of phytoplankton and bacteria in Antarctic coastal waters through impaired carbon uptake, the complex interaction of other controlling factors such as NOx availability and heterotrophic nanoflagellate abundances may modify net production responses.

To improve our understanding of OA effects on the Antarctic marine microbial loop, the roles of microzooplankton grazing (Pearce et al., 2010) and viral attack (Brussaard et al., 2013) in controlling net population balance require clarification. These components of the microbial loop may have important influences on the fate of carbon once it has initially been fixed (Ducklow et al., 2001; Suttle, 2005; Deppeler and Davidson, 2017). Measurements of bacterial extracellular enzymes (Maas et al., 2013) are also required to give insight into the potential for remineralisation of organic matter, and thus carbon export under elevated CO_2 (Piontek et al., 2013). Finally, the interactive effects of CO_2 with other factors predicted to vary with climate change require investigation (*i.e.* temperature, iron, macronutrients, light). A collapsed factorial design similar to that utilised by Boyd et al. (2015) may

provide good insight into future ocean conditions.

Acknowledgements

This work was supported by Australian Antarctic Science grants #40 and #4026 at the Australian Antarctic Division, and the Australian Government's Cooperative Research Centre Program through the Antarctic Climate and Ecosystems Cooperative Research Centre (ACE CRC). We are grateful to Dr. Bronte Tilbrook and Kate Berry for analysis of dissolved inorganic carbon and total alkalinity at CSIRO Marine and Atmospheric Research Laboratories in Hobart. We also thank and Dr. Imojen Pearce and Greg Cawthray for method development and laboratory support, and the Davis infrastructure team for the location and set-up of the minicosm reefer, in particular Mark Pekin, Shane M^{c}Evoy and Ashley Pym. We thank two anonymous referees for their helpful comments.

References

Alldredge, A.L., Gotschalk, C., Passow, U., Riebesell, U., 1995. Mass aggregation of diatom blooms: insights from a mesocosm study. Deep-Sea Res. II 42, 9–27.

Allgaier, M., Riebesell, U., Vogt, M., Thyrhaug, R., Grossart, H.P., 2008. Coupling of heterotrophic bacteria to phytoplankton bloom development at different pCO_2 levels: a mesocosm study. Biogeosciences 5, 1007–1022.

Beardall, J., Griffiths, H., Raven, J.A., 1982. Carbon isotope discrimination and the CO_2 accumulating mechanism in *Chlorella emersonii*. J. Exp. Bot. 33, 729–737.

Beardall, J., Roberts, S., Millhouse, J., 1991. Effects of nitrogen limitation on inorganic carbon uptake and specific activity of ribulose-1,5-P_2 carboxylase in green microalgae. Can. J. Bot. 69, 1146–1150.

Bell, G., Gonzalez, A., 2011. Adaptation and evolutionary rescue in metapopulations experiencing environmental deterioration. Science 332, 1327–1330.

Bellerby, R.G.J., Schulz, K.G., Riebesell, U., Neill, C., Nondal, G., Heegaard, E., Johannessen, T., Brown, K.R., 2008. Marine ecosystem community carbon and nutrient uptake stoichiometry under varying ocean acidification during the PeECE III experiment. Biogeosciences 5, 1517–1527.

Blain, S., Quéguiner, B., Armand, L., Belviso, S., Bombled, V., Bopp, L., Bowie, A., Brunet, C., Brussaard, C., Carlotti, F., Christaki, U., Corbière, A., Durand, I., Ebersbach, F., Fuda, J.-L., Garcia, N., Gerringa, L., Griffiths, B., Guigue, C., Guillerm, C., Jacquet, S., Jeandel, C., Laan, P., Lefèvre, D., Lo Monaco, C., Malits, A., Mosseri, J., Obernosterer, I., Park, Y.-H., Picheral, M., Pondaven, P., Remenyi, T., Sandroni, V., Sarthou, G., Savoye, N., Scouarnec, L., Souhaut, M., Thuiller, D., Timmermans, K., Trull, T., Uitz, J., van Beek, P., Veldhuis, M., Vincent, D., Viollier, E., Vong, L., Wagener, T., 2007. Effect of natural iron fertilization on carbon sequestration in the Southern Ocean. Nature 446, 1070–1074.

Boyd, P.W., 2011. Beyond ocean acidification. Nat. Geosci. 4, 273–274.

Boyd, C.M., Heyraud, M., Boyd, C.N., 1984. Feeding of the Antarctic krill *Euphausia superba*. J. Crustac. Biol. 4, 123–141.

Boyd, P.W., Watson, A., Law, C.S., Abraham, E., Trull, T., Murdoch, R., Baker, D.C.E., Bowie, A.R., Charette, M., Groot, P., Downing, K., Frew, R., Gall, M., Hadfield, M., Hall, J., Harvey, M., Jameson, G., La Roche, J., Liddicoat, M., Ling, R., Maldonado, M., McKay, R.M., Nodder, S., Pickmere, S., Pridmore, R., Rintoul, S., Safi, K., Sutton, P., Strzepek, R., Tanneberger, K., Turner, S., Waite, A., Zeldis, J., 2000. A mesoscale phytoplankton bloom in the polar Southern Ocean stimulated by Fe fertilization. Nature 407, 695–702.

Boyd, P.W., Strzepek, R., Chiswell, S., Chang, H., DeBruyn, J.M., Ellwood, M., Keenan, S., King, A.L., Maas, E.W., Nodder, S., Sander, S.G., Sutton, P., Twining, B.S., Wilhelm, S.W., Hutchins, D.A., 2012. Microbial control of diatom bloom dynamics in the open ocean. Geophys. Res. Lett. 39, L18601. http://dx.doi.org/10.1029/2012GL053448.

Boyd, P.W., Dillingham, P.W., McGraw, C.M., Armstrong, E.A., Cornwall, C.E., Feng, Y.-Y., Hurd, C.L., Gault-Ringold, M., Roleda, M.Y., Timmins-Schiffman, E., Nunn, B.L., 2015. Physiological responses of a Southern Ocean diatom to complex future ocean conditions. Nat. Clim. Chang. 6, 207–213. http://dx.doi.org/10.1038/NCLIMATE2811.

Brussaard, C.P.D., Noordeloos, A.A.M., Witte, H., Collenteur, M.C.J., Schulz, K., Ludwig, A., Riebesell, U., 2013. Arctic microbial community dynamics influenced by elevated CO_2 levels. Biogeosciences 10, 719–731.

Caldeira, K., Wickett, M.E., 2003. Anthropogenic carbon and ocean pH. Nature 425, 365.

Caron, D.A., Hutchins, D.A., 2013. The effect of changing climate on microzooplankton grazing and community structure; drivers, predictions and knowledge gaps. J. Plankton Res. 35 (2), 235–252.

Coale, K.H., Johnson, K.S., Chavez, F.P., Buesseler, K.O., Barber, R.T., Brzezinski, M.A., Cochlan, W.P., Millero, F.J., Falkowski, P.G., Bauer, J.E., Wanninkhof, R.H., Kudela, R.M., Altabet, M.A., Hales, B.E., Takahashi, T., Landry, M.R., Bidigare, R.R., Wang, X.J., Chase, Z., Strutton, P.G., Friederich, G.E., Gorbunov, M.Y., Lance, V.P., Hilting, A.K., Hiscock, M.R., Demarest, M., Hiscock, W.T., Sullivan, K.F., Tanner, S.J., Gordon, R.M., Hunter, C.N., Elrod, V.A., Fitzwater, S.E., Jones, J.L., Tozzi, S., Koblizek, M., Roberts, A.E., Herndon, J., Brewster, J., Ladizinsky, N., Smith, G., Cooper, D., Timothy, D., Brown, S.L., Selph, K.E., Sheridan, C.C., Twining, B.S., Johnson, Z.I., 2004. Southern ocean iron enrichment experiment: carbon cycling in high- and low-Si waters. Science 304, 408–414.

Constable, A.J., Melbourne-Thomas, J., Corney, S.P., Arrigo, K.R., Barbraud, C., Barnes, D.K.A., Bindoff, N.L., Boyd, P.W., Brandt, A., Costa, D.P., Davidson, A.T., Ducklow, H.W., Emmerson, L., Fukuchi, M., Gutt, J., Hindell, M.A., Hofmann, E.E., Hosie, G.W., Iida, T., Jacob, S., Johnston, N.M., Kawaguchi, S., Kokubun, N., Koubbi, P., Lea, M.-A., Makhado, A., Massom, R.A., Meiners, K., Meredith, M.P., Murphy, E.J., Nicol, S., Reid, K., Richerson, K., Riddle, M.J., Rintoul, S.R., Smith Jr, W.O., Southwell, C., Stark, J.S., Sumner, M., Swadling, K.M., Takahashi, K.T., Trathan, P.N., Welsford, D.C., Weimerskirch, H., Westwood, K.J., Wienecke, B.C., Wolf-Gladrow, D., Wright, S.W., Xavier, J.C., Ziegler, P., 2014. Climate change and Southern Ocean ecosystems I: how changes in physical habitats directly affect marine biota. Glob. Chang. Biol. 20, 3004–3025. http://dx.doi.org/10.1111/gcb.12623.

Davidson, A.T., McKinlay, J., Westwood, K., Thomson, P.G., van den Enden, R., de Salas, M., Wright, S., Berry, K., Tilbrook, B., 2016. Enhanced CO_2 concentrations change the structure and function of Antarctic marine microbial communities. Mar. Ecol. Prog. Ser. 552, 93–113. http://dx.doi.org/10.3354/meps11742.

Delille, B., Harlay, J., Zondervan, I., Jacquet, S., Chou, L., Wollast, R., Bellerby, R.G.J., Frankignoulle, M., Borges, A.V., Riebesell, U., Gattuso, J.P., 2005. Response of primary production and calcification to changes of pCO_2 during experimental blooms of the coccolithophorid *Emiliania huxleyi*. Glob. Biogeochem. Cycles 19, GB2023. http://dx.doi.org/10.1029/2004GB002318.

Deppeler, S.L., Davidson, A.T., 2017. Southern Ocean phytoplankton in a changing climate. Front. Mar. Sci. 4, 40. http://dx.doi.org/10.3389/fmars.2017.00040.

Deppeler, S.L., Petrou, K., Schulz, K., Westwood, K., Pearce, I., McKinlay, J., Davidson, A. (in review). Ocean acidification of a coastal Antarctic marine microbial community reveals a critical threshold for CO_2 tolerance in phytoplankton productivity. Biogeosci. Discuss., https://doi.org/doi.org/10.5194/bg-2017-226.

DeVries, T., 2014. The oceanic anthropogenic CO_2 sink: storage, air-sea fluxes, and transports over the industrial era. Glob. Biogeochem. Cycles 28, 631–647. http://dx.doi.org/10.1002/2013GB004739.

Ducklow, H.W., Steinberg, D.K., Buesseler, K.O., 2001. Upper ocean carbon export and the biological pump. Oceanography 14, 50–58.

Efremov, R.G., Baradaran, R., Sazanov, L., 2010. The architecture of respiratory complex I. Nature 465, 441–445. http://dx.doi.org/10.1038/nature09066.

Egge, J.K., Thingstad, T.F., Larsen, A., Engel, A., Wohlers, J., Bellerby, R.G.J., Riebesell, U., 2009. Primary production during nutrient-induced blooms at elevated CO_2 concentrations. Biogeosciences 6, 877–885.

Engel, A., 2002. Direct relationship between CO_2 uptake and transparent exopolymer particle production in natural phytoplankton. J. Plankton Res. 24, 49–53.

Engel, A., Borchard, C., Piontek, J., Schulz, K.G., Riebesell, U., Bellerby, R., 2013. CO_2 increases ^{14}C primary production in an Arctic plankton community. Biogeosciences 10, 1291–1308.

Erdner, D.L., Price, N.M., Doucette, G.J., Peleato, M.L., Anderson, D.M., 1999. Characterization of ferredoxin and flavodoxin as markers of iron limitation in marine phytoplankton. Mar. Ecol. Prog. Ser. 184, 43–53.

Finkel, Z.V., Beardall, J., Flynn, K.J., Quigg, A., Alwyn, T., Rees, V., Raven, J.A., 2010. Phytoplankton in a changing world: cell size and elemental stoichiometry. J. Plankton Res. 32 (1), 119–137.

Fogg, G.E., 1966. The extracellular products of algae. Oceanogr. Mar. Biol. Annu. Rev. 4, 195–212.

Gao, K., Xu, J., Gao, G., Li, Y., Hutchins, D.A., Huang, B., Wang, L., Zheng, Y., Jin, P., Cai, X., Häder, D.-P., Li, W., Xu, K., Liu, N., Riebesell, U., 2012. Rising CO_2 and increased light exposure synergistically reduce marine primary productivity. Nat. Clim. Chang. 2, 519–523. http://dx.doi.org/10.1038/NCLIMATE1507.

Gattuso, J.P., Hansson, L., 2011. Ocean acidification: background and history. In: Gattuso, J.P., Hansson, L. (Eds.), Ocean Acidification. Oxford University Press, Oxford, pp. 1–20.

Gervais, F., Riebesell, U., Gorbunov, N.Y., 2002. Changes in size-fractionated primary productivity and chlorophyll *a* in response to iron fertilization in the southern polar frontal zone. Limnol. Oceanogr. 47, 1324–1335.

Gibson, J.E., 1998. Carbon flow through inshore marine environments of the Vestfold Hills, East Antarctica. In: ANARE Report 139. Australian Antarctic Division, Commonwealth of Australia, pp. 45–46.

Gibson, J.A.E., Trull, T.W., 1999. Annual cycle of fCO_2 under sea-ice and in open water in Prydz Bay, East Antarctica. Mar. Chem. 66, 187–200.

Giordano, M., Beardall, J., Raven, J.A., 2005. CO_2 concentrating mechanisms in algae: mechanisms environmental modulation, and evolution. Annu. Rev. Plant Biol. 56, 99–131.

Gleitz, M., Rutgers van der Loeff, M., Thomas, D.N., Dieckmann, G., Millero, F.J., 1995. Comparison of summer and winter inorganic carbon, oxygen and nutrient concentrations in Antarctic sea-ice brine. Mar. Chem. 51, 81–91.

Grossart, H.P., Allgaier, M., Passow, U., Riebesell, U., 2006. Testing the effect of CO_2 concentration on the dynamics of marine heterotrophic bacterioplankton. Limnol. Oceanogr. 51 (1), 1–11.

Hassler, C.S., Schoemann, V., 2009. Bioavailability of organically bound Fe to model phytoplankton of the Southern Ocean. Biogeosciences 6, 2281–2296.

Hein, M., Sand-Jensen, K., 1997. CO_2 increases oceanic primary production. Nature 388, 526–527.

Hoppe, C.J.M., Hassler, C.S., Payne, C.D., Tortell, P.D., Rost, B., Trimborn, S., 2013. Iron limitation modulates ocean acidification effects on Southern Ocean phytoplankton communities. PLoS One 8 (11), e79890. http://dx.doi.org/10.1371/journal.Pone.0079890.

Hoppe, C.J.M., Holtz, L.-M., Trimborn, S., Rost, B., 2015. Ocean acidification decreases the light-use efficiency in an Antarctic diatom under dynamic but not constant light. New Phytol. 207, 159–171. http://dx.doi.org/10.1111/nph.13334.

Hurd, C.L., Hepburn, C.D., Currie, K.I., Raven, J.A., Hunter, K.A., 2009. Testing the effects of ocean acidification on algal metabolism: considerations for experimental designs.

J. Phycol. 45 (6), 1236–1251.
Kawaguchi, S., Ichii, T., Haganobu, M., 1999. Green krill, the indicator of micro- and nano-sized phytoplankton availability to krill. Polar Biol. 22, 133–136.
Kim, J.M., Lee, K., Shin, K., Yang, E.J., Engel, A., Karl, D.M., Kim, H.C., 2011. Shifts in biogenic carbon flow from particulate to dissolved forms under high carbon dioxide and warm ocean conditions. Geophys. Res. Lett. 38, L08612. http://dx.doi.org/10.1029/2011GL047346.
Kirchman, D., 2001. Measuring bacterial biomass production and growth rates from leucine incorporation in natural aquatic environments. Methods Microbiol. 30, 227–237.
Kirchman, D.L., Suzuki, Y., Garside, C., Ducklow, H.W., 1991. High turnover rates of dissolved organic carbon during a spring phytoplankton bloom. Nature 352, 612–614.
de Kluijver, A., Soetaert, K., Schulz, K.G., Riebesell, U., Bellerby, R.G.J., Middelburg, J.J., 2010. Phytoplankton-bacteria coupling under elevated CO_2 levels: a stable isotope labeling study. Biogeosciences 7, 3783–3797.
Kranz, S.A., Young, J.N., Hopkinson, B.M., Goldman, J.A.L., Tortell, P.D., Morel, F.M.M., 2015. Low temperature reduces the energetic requirement for the CO_2 concentrating mechanism in diatoms. New Phytol. 205, 192–201. http://dx.doi.org/10.1111/nph.12976.
Kruskopf, M., Flynn, K.J., 2006. Chlorophyll content and fluorescence responses cannot be used to gauge reliably phytoplankton biomass, nutrient status or growth rate. New Phytol. 169, 525–536.
Laws, E.A., 1991. Photosynthetic quotients, new production and net community production. Deep-Sea Res. I 38, 143–167.
Li, G., Campbell, D.A., 2013. Rising CO_2 interacts with growth light and growth rate to alter photosystem II photoinactivation of the coastal diatom *Thalassiosira pseudonana*. PLoS One 8, e55562.
Liu, J., Weinbauer, M.G., Maier, C., Dai, M., Gattuso, J.P., 2010. Effect of ocean acidification on microbial diversity and on microbe-driven biogeochemistry and ecosystem functioning. Aquat. Microb. Ecol. 61, 291–305. http://dx.doi.org/10.3354/ame01446.
Lohbeck, K.T., Riebesell, U., Reusch, T.B.H., 2012. Adaptive evolution of a key phytoplankton species to ocean acidification. Nat. Geosci. 5, 346–351.
Maas, E.W., Law, C.S., Hall, J.A., Pickmere, S., Currie, K.I., Chang, F.H., Voyles, K.M., Caird, D., 2013. Effect of ocean acidification on bacterial abundance, activity and diversity in the Ross Sea, Antarctica. Aquat. Microb. Ecol. 70, 1–15. http://dx.doi.org/10.3354/ame01633.
Mackey, K.R.M., Morris, J.J., Morel, F.M.M., Kranz, S.A., 2015. Response of photosynthesis to ocean acidification. Oceanography 28 (2), 74–91. http://dx.doi.org/10.5670/oceanog.2015.33.
Marie, D., Brussaard, C.P., Thyrhaug, R., Bratbak, G., Vaulot, D., 1999. Enumeration of marine viruses in culture and natural samples by flow cytometry. Appl. Environ. Microbiol. 65, 45–52.
Matear, R.J., Hirst, A.C., 1999. Climate change feedback on the future oceanic CO_2 uptake. Tellus 51, 722–733.
Nicol, S., Meiners, K., Raymond, B., 2010. BROKE-West, a large ecosystem survey of the south West Indian Ocean sector of the Southern Ocean, 30°E–80°E (CCAMLR division 58.4.2). Deep-Sea Res. II 57, 693–700.
Pearce, I., Davidson, A.T., Bell, E.M., Wright, S., 2007. Seasonal changes in the concentration and metabolic activity of bacteria and viruses at an Antarctic coastal site. Aquat. Microb. Ecol. 47, 11–23.
Pearce, I., Davidson, A.T., Thomson, P., Wright, S., van den Enden, R., 2010. Marine microbial ecology off East Antarctica (30°–80°E): rates of bacterial and phytoplankton growth and grazing by heterotrophic protists. Deep-Sea Res. II 57, 849–862.
Peloquin, J., Hall, J., Safi, K., Smith, W.O., Wright, S., van den Enden, R., 2010. The response of phytoplankton to iron enrichment in sub-Antarctic HNLC L Si waters: results from the SAGE experiment. Deep-Sea Res. II 58 (6), 808–823. http://dx.doi.org/10.1016/j.dsr2.2010.10.021.
Petrou, K., Kranz, S.A., Trimborn, S., Hassler, C.S., Ameijeiras, S.B., Sackett, O., Ralph, P.J., Davidson, A.T., 2016. Southern Ocean phytoplankton physiology in a changing climate. J. Plant Physiol. 203, 135–150. http://dx.doi.org/10.1016/j.jplph.2016.05.004.
Piontek, J., Borchard, C., Sperling, M., Schulz, K.G., Riebesell, U., Engel, A., 2013. Response of bacterioplankton activity in an Arctic fjord system to elevated pCO_2: results from a mesocosm perturbation study. Biogeosciences 10, 297–314.
Platt, T., Gallegos, C.L., Harrison, W.G., 1980. Photoinhibition of photosynthesis in natural assemblages of marine phytoplankton. J. Mar. Res. 38, 687–701.
Raven, J.A., Giordano, M., Beardall, J., Maberly, S.C., 2012. Algal evolution in relation to atmospheric CO_2: carboxylases, carbon concentrating mechanisms and carbon oxidation cycles. Philos. Trans. R. Soc. B 367, 493–507. http://dx.doi.org/10.1098/rstb.2011.0212.
Redfield, A.C., 1958. The biological control of chemical factors in the environment. Am. Sci. 46, 205–221.
Riebesell, U., Schulz, K.G., Bellerby, R.G.J., Botros, M., Fritsche, P., Meyerhöfer, M., Neill, C., Nondal, G., Oschlies, A., Wohlers, J., Zöllner, E., 2007. Enhanced biological carbon consumption in a high CO_2 ocean. Nature 450, 545–549.
Riebesell, U., Bellerby, R.G.J., Grossart, H.P., Thingstad, F., 2008. Mesocosm CO_2 perturbation studies: from organism to community level. Biogeosciences 5, 1157–1164.
Riebesell, U., Fabry, V.J., Hansson, L., Gattuso, J.P., 2010. Guide to Best Practices for Ocean Acidification Research and Data Reporting. Publications Office of the European Union, Luxembourg.
Riebesell, U., Gattuso, J.P., Thingstad, T.F., Middelburg, J.J., 2013. Arctic ocean acidification: pelagic ecosystem and biogeochemical responses during a mesocosm study. Biogeosciences 10, 5619–5626.
Riley, G.A., 1957. Phytoplankton of the North Central Sargasso Sea, 1950–52. Limnol. Oceanogr. 2, 252–270.
Roden, N.P., Shadwick, E.H., Tilbrook, B., Trull, T.W., 2013. Annual cycle of carbonate chemistry and decadal change in coastal Prydz Bay, East Antarctica. Mar. Chem. 155, 135–147.
Sallée, J.B., Speer, K.G., Rintoul, S.R., 2010. Zonally asymmetric response of the Southern Ocean mixed-layer depth to the Southern Annular Mode. Nat. Geosci. 3, 273–279. http://dx.doi.org/10.1038/NGE0812.
Sarmiento, J.L., Slater, R., Barber, R., Bopp, L., Doney, S.C., Hirst, A.C., Kleypas, J., Matear, R., Mikolajewicz, U., Monfray, P., Soldatov, V., Spall, S.A., Stouffer, R., 2004. Response of ocean ecosystems to climate warming. Glob. Biogeochem. Cycles 18, GB3003.
Schaum, E., Rost, B., Millar, A.J., Collins, S., 2013. Variation in plastic responses of a globally distributed picoplankton species to ocean acidification. Nat. Clim. Chang. 3, 298–302.
Schulz, K.G., Bellerby, R.G.J., Brussaard, C.P.D., Büdenbender, J., Czerny, J., Engel, A., Fischer, M., Koch-Klavsen, S., Krug, S.A., Lischka, S., Ludwig, A., Meyerhöfer, M., Nondal, G., Silyakova, A., Stuhr, A., Riebesell, U., 2013. Temporal biomass dynamics of an Arctic plankton bloom in response to increasing levels of atmospheric carbon dioxide. Biogeosciences 10, 161–180.
Scott, F.J., Davidson, A.T., Marchant, H.J., 2000. Seasonal variation in plankton, submicrometre particles, and size-fractionated dissolved organic carbon in Antarctic coastal waters. Polar Biol. 23, 635–643.
Shi, D., Xu, Y., Hopkinson, B.M., Morel, F.M.M., 2010. Effect of ocean acidification on iron availability to marine phytoplankton. Science 327, 676–679.
Smith, D.C., Azam, F., 1992. A simple economical method for measuring bacterial protein synthesis rates in sea water using ^{3}H-leucine. Mar. Microb. Food Webs 6, 107–109.
Sugie, K., Yoshimura, T., 2016. Effects of high CO_2 levels on the ecophysiology of the diatom *Thalassiosira weissflogii* differ depending on the iron nutritional status. ICES J. Mar. Sci. 73 (3), 680–692.
Sugie, K., Endo, H., Suzuki, K., Nishioka, J., Kiyosawa, H., Yoshimura, T., 2013. Synergistic effects of pCO2 and iron availability on nutrient consumption ratio of the Bering sea phytoplankton community. Biogeosciences 10, 6309–6321.
Sunda, W.G., Huntsman, S.A., 1997. Interrelated influence of iron, light and cell size on marine phytoplankton growth. Nature 390, 389–392.
Suttle, C.A., 2005. Viruses in the sea. Nature 437, 356–361. http://dx.doi.org/10.1038/nature04160.
Tanaka, T., Alliouane, S., Bellerby, R.G.B., Czerny, J., de Kluijver, A., Riebesell, U., Schulz, K.G., Silyakova, A., Gattuso, J.P., 2013. Effect of increased pCO_2 on the planktonic metabolism balance during a mesocosm experiment in an Arctic fjord. Biogeosciences 10, 315–325.
Thingstad, T.F., Bellerby, R.G.J., Bratbak, G., Børsheim, K.Y., Egge, J.K., Heldal, M., Larsen, A., Neill, C., Nejstgaard, J., Norland, S., Sandaa, R.A., Skjoldal, E.F., Tanaka, T., Thyrhaug, R., Töpper, B., 2008. Counterintuitive carbon-to-nutrient coupling in an Arctic pelagic ecosystem. Nature 455, 387–390.
Thomson, P.G., Davidson, A.T., Maher, L., 2016. Increasing pCO_2 changes community composition of pico- and nano-sized protists and prokaryotes at a coastal Antarctic site. Mar. Ecol. Prog. Ser. 554, 51–69. http://dx.doi.org/10.3354/meps11803.
Tipton, K.F., Dixon, H.B., 1979. Effects of pH on enzymes. Methods Enymol. 63, 183–234.
Toggweiler, J.R., 1993. Carbon overconsumption. Nature 363, 210–211.
Tortell, P.D., Payne, C.D., Li, Y., Trimborn, S., Rost, B., Smith, W.O., Riesselman, C., Dunbar, R.B., Sedwick, P., DiTullio, D., 2008. CO_2 sensitivity of Southern Ocean phytoplankton. Geophys. Res. Lett. 35, L04605. http://dx.doi.org/10.1029/2007GL032583.
Tortell, P.D., Asher, E.C., Ducklow, H.W., Goldman, J.A.L., Dacey, J.W.H., Grzymski, J.J., Young, J.N., Kranz, S.A., Bernard, K.S., Morel, F.M.M., 2014. Metabolic balance of coastal Antarctic waters revealed by autonomous pCO_2 and ΔO_2/Ar measurements. Geophys. Res. Lett. 41, 6803–6810. http://dx.doi.org/10.1002/2014GL061266.
Trimborn, S., Brenneis, T., Sweet, E., Rost, B., 2013. Sensitivity of Antarctic phytoplankton species to ocean acidification: growth, carbon acquisition, and species interaction. Limnol. Oceanogr. 58 (3), 997–1007.
Trimborn, S., Thoms, S., Brenneis, T., Heiden, J.P., Beszteri, S., Bischof, K., 2017. Two Southern Ocean diatoms are more sensitive to ocean acidification and changes in irradiance than the prymnesiophyte *Phaeocystis antarctica*. Physiol. Plant. http://dx.doi.org/10.1111/ppl.12539.
Westwood, K.J., Griffiths, F.B., Meiners, K.M., Williams, G.D., 2010. Primary productivity off the Antarctic coast from 30°–80°E; BROKE-West survey, 2006. Deep-Sea Res. II 57, 794–814.
Westwood, K.J., Griffiths, F.B., Webb, J.P., Wright, S.W., 2011. Primary production in the sub-Antarctic and polar frontal zones south of Tasmania, Australia; SAZ-sense survey, 2007. Deep-Sea Res. II 58, 2162–2178.
Wright, S.W., van den Enden, R.L., Pearce, I., Davidson, A.T., Scott, F.J., Westwood, K.J., 2010. Phytoplankton community structure and stocks in the Southern Ocean (30°–80°E) determined by CHEMTAX analysis of HPLC pigment signatures. Deep-Sea Res. II 57, 758–778.
Young, E.B., Beardall, J., 2005. Modulation of photosynthesis and inorganic carbon acquisition in a marine microalga by nitrogen, iron and light availability. Can. J. Bot. 83 (7), 917–928.
Young, J.N., Kranz, S.A., Goldman, J.A.L., Tortell, P.D., Morel, F.M.M., 2015. Antarctic phytoplankton down-regulate their carbon-concentrating mechanisms under high CO_2 with no change in growth rates. Mar. Ecol. Prog. Ser. 532, 13–28.